

## **Antiangiogenic effect of circulating extracellular vesicles in acute coronary syndrome: role of miR-199a-3p and miR-125a-5p**

**Short Title:** Circulating EVs and angiogenesis in ACS

Joaquin Bobi<sup>1,2\*</sup>, Francisco-Rafael Jimenez-Trinidad<sup>1,3\*</sup>, Luis Ortega-Paz<sup>1,2</sup>, Nuria Cortes-Serra<sup>5,6</sup>, Iolanda Lazaro<sup>1</sup>, Juan-Jose Rodriguez<sup>2</sup>, Carmen Fernandez-Becerra<sup>5,6,7</sup>, Ana García-Álvarez<sup>1,2,4</sup>, Manel Sabate<sup>1,2</sup>, Salvatore Brugaletta<sup>1,2</sup>, Ana-Paula Dantas<sup>1,2,3</sup>.

1. Institute of Biomedical Research August Pi Sunyer (IDIBAPS), Barcelona, Spain
2. Institut Clínic Cardiovascular (ICCV), Hospital Clínic, Barcelona, Spain.
3. Department of Biomedicine, School of Medicine and Health Sciences, University of Barcelona, Spain
4. Centro Nacional de Investigaciones Cardiovasculares, Madrid, Spain.
5. ISGlobal, Barcelona Institute for Global Health, Facultat de Medicina i Ciències de la Salut, Universitat de Barcelona (UB), Barcelona, Spain
6. IGTP Institut d'Investigació Germans Trias I Pujol, Badalona, Barcelona, Spain
7. CIBERINFEC, ISCIII - CIBER de Enfermedades Infecciosas, Instituto de Salud Carlos III, Majadahonda, Madrid, Spain

*\*Equal contribution*

### **Correspondence:**

Ana Paula Dantas. Experimental Cardiology. Institut d'Investigacions Biomèdiques August Pi i Sunyer (IDIBAPS). C/ Casanova 143. Cellex, Planta 2 Sector A. 08036, Barcelona, Spain.

Tel: +34 932274500 Ext 4899. [apvilleladantas@ub.edu](mailto:apvilleladantas@ub.edu)

**Word Count:** Total (6860 words), Abstract (260 words), 39 References, 5 Figures, 1, graphic abstract  
2 Table, 3 supplementary materials.

## **Abstract**

**Objective:** Circulating extracellular vesicles (EVs) have a great impact on human health as a biomarker and messengers in intercellular signaling. We aimed to determine how miRNA profile of circulating EVs during an acute coronary event interferes with the vasculogenic potential of endothelial cells (EC).

**Approach and Results:** EVs were purified from plasma of patients in the acute phase of non-ST segment elevation myocardial infarction (NSTEMI, n=33), and from healthy donors (n=19) used as control group. Human ECs were treated with EV suspension ( $5 \times 10^7$  particles/cm<sup>2</sup>) and tested for their vasculogenic potential and mRNA expression. EV's miRNA profile was determined by miRNA array. EVs levels were markedly increased in the plasma of NSTEMI ( $2.3 \times 10^{11} \pm 1.5 \times 10^{10}$  particles/ml) vs control ( $1.2 \times 10^{11} \pm 1.1 \times 10^{10}$  particles/ml; p=0.02). Treatment of ECs with control EVs increased migration, tube formation, and shaped more branched vessel-like structures in comparison to Sham-treated ECs. Nevertheless, EVs from NSTEMI lacked their vasculogenic potential. Network analysis of EV miRNA and EC mRNA expression revealed a correlation of increased miR-199a-3p and miR-125a-5p expression with a decrease of components involved in EC sprout and stabilization. Combined therapy with miR-199a-3p and miR-125a-5p decreased ECs vasculogenic potential. Moreover, anti-miRNA therapy with combination of anti-miR-125a-5p and anti-miR-anti-199a-3p restore vasculogenic potential impaired by NSTEMI EVs.

**Conclusions:** Circulating EVs play an important role in the control of angiogenesis. However, in the acute phase of NSTEMI, intercellular communication via EV is modified and loses their ability to generate new blood vessels. The loss of angiogenic capacity of EVs during NSTEMI may be an important player in the disease progression and outcomes.

**Keywords:** Extracellular vesicles, angiogenesis, miRNA profile, acute coronary syndrome.

## Abbreviations

<b>ALIX</b>	Programmed cell death 6 interacting protein
<b>ANG</b>	Angiogenin
<b>Ang1 / Angpt1</b>	Angiopoietin 1
<b>Ang2 / Angpt2</b>	Angiopoietin 2
<b>ANXA5</b>	Annexin A5
<b>ARTN</b>	Artemin
<b>CD44</b>	Inlu-related p80 glycoprotein
<b>CD63</b>	Tetraspanin, CD 63 antigen
<b>CD81</b>	Tetraspanin, CD81 antigen
<b>CD9</b>	Tetraspanin, CD9 antigen
<b>COL4A1</b>	Collagen, type iv, alpha-1
<b>COL4A2</b>	Collagen, type iv, alpha-2
<b>COL4A5</b>	Collagen, type iv, alpha-5
<b>CYP1A2</b>	Cytochrome p450, subfamily i, polypeptide 2
<b>DPPIV (DPP4)</b>	Dipeptidyl peptidase iv; dpp4
<b>EC</b>	Endothelial cells
<b>EpCam</b>	Epithelial cell adhesion molecule; often found in cancer-derived exosomes
<b>eNOS</b>	Endothelial nitric oxide synthase
<b>ET-1</b>	Endothelin-1
<b>EVs</b>	Extracellular vesicles
<b>FDR</b>	False discovery rate
<b>FLOT1</b>	Flotillin-1
<b>FLT1 (VEGFR1)</b>	Vascular endothelial growth factor receptor 1
<b>GM130</b>	Cis-golgi matrix protein
<b>HUVEC</b>	Human umbilical vein endothelial cells
<b>ICAM1</b>	Intercellular adhesion molecule 1
<b>IGFBP-1</b>	Insulin-like growth factor-binding protein 1
<b>IGFBP-3</b>	Insulin-like growth factor-binding protein 3
<b>IL1A</b>	Interleukin 1-alpha
<b>ITGAV</b>	Integrin, alpha-v
<b>KDR (VEGFR2)</b>	Vascular endothelial growth factor receptor 2
<b>MMP-9</b>	Matrix metalloproteinase 9
<b>MMP2</b>	Matrix metalloproteinase 2
<b>NSTEMI</b>	Non-ST segment elevation myocardial infarction
<b>PAI-1</b>	Serpin E1
<b>PCI</b>	Percutaneous coronary intervention
<b>PDGF</b>	Platelet-derived growth factor
<b>PDGFB</b>	Platelet-derived growth factor, beta polypeptide
<b>PEDF</b>	Serpin F1
<b>PF4</b>	Platelet factor 4
<b>PTGS2</b>	Cyclooxygenase 2
<b>SEC</b>	Size exclusion chromatography

<b>SKI</b>	Sk oncogene
<b>STAT3</b>	Signal transducer and activator of transcription 3
<b>TIE1</b>	Protein receptor tyrosine kinase tie 1
<b>TIMP-1</b>	Tissue inhibitor of metalloproteinase 1
<b>TSG101</b>	Tumor susceptibility gene 101
<b>TSP-1</b>	Thrombospondin-1
<b>VEGF</b>	Vascular endothelial growth factor

## 1 **Introduction**

2 Intercellular communication plays a pivotal role in cardiovascular physiology, regulating the  
3 function of cardiac and vascular tissues in both health and disease. Cardiovascular cells not only  
4 regulate their own conduct, but they are also interconnected with other cells to ensure their correct  
5 behavior. This communication occurs in many forms, ranging from localized ion exchange, release of  
6 biochemical messengers to the exchange of extracellular vesicles as vectors of biological information  
7 [1, 2]. Extracellular vesicles (EVs) are a heterogenous group of membrane-bound particles released by  
8 cells into the extracellular environment loaded with a specific cargo of proteins and nucleic acids (DNA  
9 fragments, mRNAs and miRNAs) from donor cells that, when captured by recipient cells, can influence  
10 and modify their phenotypes [2]. They are highly stable in body fluids, and therefore, intercellular  
11 signaling via EVs can be shuttled across cardiovascular cells in a paracrine or endocrine manner to  
12 either maintain homeostasis or elicit the onset and progression of cardiovascular disease (CVD) [2].

13 Growing evidence convincingly indicates that circulating levels and the specific molecular  
14 profiles of EVs are significantly influenced by cardiovascular risk factors, playing an essential role in  
15 the progression of CVD. For example, distinct expressions of miRNAs within EVs can trigger  
16 inflammation, contribute to endothelial dysfunction, and promote the progression and instability of  
17 atherosclerotic plaques. [3, 4]. Furthermore, EV-associated miRNAs have been identified as promising  
18 biomarkers for the early detection and prognosis of coronary artery disease, and as potential  
19 therapeutic targets for more effective and tailored modulation of disease progression [5].

20 In the past years, EVs released by different cell types have been pointed as important  
21 mediators of angiogenesis, raising particular interest in acute coronary syndromes [6]. The heart can  
22 become, for example, less sensitive to new episodes of ischemia if sufficiently supplied by blood flow  
23 through well-developed collateral coronary vessels. In this regard, effective signaling towards  
24 angiogenesis in the heart can subsequently induce growth, expansion, and remodeling of primitive  
25 vessels into a complex and mature vascular network, decreasing the risk of a reinfarction [7].  
26 Angiogenesis is also required after an acute myocardial infarction (AMI) event to form functional  
27 capillary networks in the periphery of the infarcted area to decrease scar and to trigger collateral  
28 growth upstream and around the occlusion site in the myocardium to attenuate damage and prevent  
29 poor cardiac outcomes [8].

30 It remains unclear, however, whether specific molecular profile of intrinsic circulating EVs  
31 during a cardiovascular event could improve or hinder the process of vascularization of the infarcted  
32 area and how they may influence patient outcomes. In this study, we aimed to increase our knowledge  
33 about the role of circulating EVs in the pathophysiology of AMI, seeking to determine how these  
34 nanovesicles released into the circulation of patients during an ongoing AMI modulate the angiogenic

1 potential of ECs. Subsequently, we evaluated whether a differential miRNA profile within EVs is  
2 translated into a modification of ECs phenotype concerning their angiogenic potential and  
3 transcriptional profile.

## 4 5 **Methods**

### 6 **Patient inclusion**

7 Consecutive patients (n=33) admitted to our Institution between May 2017 and September  
8 2018 owing to a non-ST-segment elevation AMI (NSTEMI) requiring percutaneous coronary  
9 intervention (PCI) were included in the study. Inclusion criteria were age  $\leq$  75 years, with a first acute  
10 coronary syndrome, and more than one traditional cardiovascular risk factor. Exclusion criteria were  
11 previously documented acute coronary syndrome or stroke, diabetes, thrombocytopenia, oral  
12 anticoagulant therapy, vasculitis, or any known immunological disorder, severe hepatic failure,  
13 uncontrolled hypertension (systolic or diastolic arterial pressure  $>180$  mmHg or  $120$ , respectively,  
14 despite medical therapy), limited life expectancy, e.g., neoplasms, others, inability to obtain informed  
15 consent, pregnancy. Diabetic patients were excluded due to metabolic variations that can interfere  
16 with EVs. A group of healthy subjects (n=19) matched by age and sex was used as a control group. All  
17 protocols were carried out under the approval of the Clinical Research Ethics Committee (CEIm) of  
18 Hospital Clinic (HCB/2016/0366), under the principles of the Declaration of Helsinki (64th General  
19 Assembly of the World Medical Association, Fortaleza, Brazil, October 2013). The patients included in  
20 the study were informed of the experimental protocols and provided signed formal consents.

### 21 22 **Extracellular vesicles isolation, characterization, and quantitation**

23 EVs were purified from 1mL aliquot of plasma by a combination of polymer-based precipitation  
24 and size exclusion chromatography (SEC), as described [9]. Fractions F6-F10 from the SEC were  
25 analyzed by flow cytometry for the presence of antigens CD9, CD63, or CD81 [9], and by a semi-  
26 quantitative antibody array with eight antibodies for known EVs markers (Exo-Check™). Particle size  
27 and distribution were characterized by nanoparticle tracking analysis using a NanoSight NS300 system,  
28 and EVs concentration in each sample was determined with FluoroCet Exosome Quantitation kit,  
29 following the manufacturer's protocol.

### 30 31 **Cell culture and EVs treatments**

32 Primary human umbilical vein endothelial (HUVEC) cell line was maintained in culture at 37°C in a  
33 humidified atmosphere at 95% air and 5% CO<sub>2</sub> in EGM-2 media supplemented with 10% (v/v) fetal  
34 bovine serum (FBS) and growth supplements. After O.N. incubation in EV-free media [EGM-2 media

1 supplemented with 5% (v/v) EV-depleted FBS], cells were individually treated with  $5 \times 10^7$  particles /  
2  $\text{cm}^2$  from fractions F7-F9 of each sample of NSTEMI patient or control volunteer. A group of cells  
3 treated with purified EVs from HUVEC culture media (n = 8) was considered as Sham treatment group,  
4 and a set of untreated cells (NT, n = 8) was used as assay controls.

### 6 **Endothelial cell phenotype**

7 Following 48 hours of incubation with EVs, changes in HUVEC phenotype were determined based  
8 on their ability to migrate and undergo angiogenesis. The migration rate of HUVEC was determined  
9 by standardized scratch assay [10]. The ability of EV-treated ECs to form capillary-like structures was  
10 determined by seeding them onto  $\mu$ -Angiogenesis Slides coated with factor-reduced Matrigel™, as  
11 described [11]. The potential of EVs in vascular morphogenesis was determined by the ability of ECs  
12 to disperse throughout a matrix and associate into microvessel-like structures (long branches and  
13 anastomoses with lumens of capillary diameter) and to interconnect to form a network. For that  
14 purpose, the behavior of HUVEC treated with EVs was tested in a 3D angiogenesis system, according  
15 to the protocol described by Nakatsu et al [12].

### 17 **miRNA and mRNA expression**

18 Total RNA (tRNA) was isolated from 100 $\mu$ l of EV solution fractions using the miRCURY RNA  
19 Isolation Kit for Biofluids, and from EV-treated ECs ( $4\text{-}5 \times 10^5$  cells) with RNeasy Mini Kit following the  
20 manufacturer's instructions. Aliquots were assessed for quality and quantity with a Qubit™  
21 Fluoremeter and Agilent 2100 Bioanalyzer. The expression of 754 unique miRNA was determined in  
22 randomly pooled EVs samples from control (n=4) and NSTEMI (n=10) by TaqMan™ OpenArray™  
23 Human Advanced MicroRNA Panel. mRNA expression of 178 genes involved in angiogenesis and  
24 vascular morphogenesis was determined in randomly pooled samples of tRNA isolated from Sham-  
25 treated HUVEC (n=4) and cells treated with EVs from control (n=4) and NSTEMI (n=4), using TaqMan™  
26 Gene Expression Array Cards. Expression of the miRNAs of interest was determined in the entire  
27 cohort by qRT-PCR with TaqMan™ microRNA Assays and QuantStudio™ PCR System. Prediction of  
28 target genes interaction with miRNA modified in EVs of NSTEMI patients was made with miRNet  
29 (<https://www.mirnet.ca/>) [13] and integrated with their molecular function using the Gene Ontology  
30 and Kyoto Encyclopedia.

### 32 **Validation of antiangiogenic effect of smiR-125a-5p and miR-199a-3p**

33 At 70-80% confluence HUVECs were transfected with miRCURY LNA miRNA mimics and inhibitors  
34 for miR-125a-5p and miR-199a-3p labeled at the 5' end with 6-FAM. A scrambled oligonucleotide

1 sequence was used as and mimic negative control. After incubation O.N., transfection media was  
2 replaced by complete endothelial cell media (described above) and cells were incubated for additional  
3 24 h before performing 3D angiogenesis assay. The effects of miRNAs on EC phenotype were studied  
4 by treating cells with miRNA alone (miR-125a-5p or miR-199a-3p) or in combination (miR-125a-5p +  
5 miR-199a-3p). To determine the effects of miRNA inhibition on the actions of NSTEMI EVs, ECs were  
6 treated with anti-miRNA (anti-miR-125a-5p, anti-miR-199a-3p or a combination of both inhibitors),  
7 along with treatments of a pull of EVs from NSTEMI patients.

## 9 **Data Analysis and Statistics**

10 Sample size was calculated based on the model  $n = 2x [(Z\alpha + Z1-\beta)^2 x (\delta)^2] / \Delta^2$  to estimate the  
11 minimum number of samples required in each experimental subgroup NSTEMI vs. control to obtain  
12 an alpha error of 5% ( $Z\alpha$ ) [two-tailed test because the results could be bidirectional], 95% power ( $Z1-$   
13  $\beta$ ) to detect approximately double exchange rate transcriptional expression between groups ( $\Delta$ ); and  
14 standard deviation levels ( $\delta$ ) of 0.7 [14]. According to their distribution, continuous variables were  
15 expressed as mean  $\pm$  standard deviation (SD) or median with interquartile range (IQR). Continuous  
16 variables were compared with unpaired and two-tailed T-tests with Welch's correction. In contrast,  
17 the chi-square or Fisher's exact test was used to compare the categorical variables, as appropriate. A  
18 comparison of means across the independent variables (Sham, Control, NSTEMI) was performed by  
19 Brown Forsythe and Welch ANOVA, followed by Dunnett's T3 posthoc analysis multiple comparisons.  
20 Repeated measure 2-way ANOVA analyzed the dependence of data of each EV marker in each SEC  
21 fraction with the two different experimental groups (Control vs NSTEMI). For miRNA and mRNA  
22 expression, the limit of quantitation (LoQ) for each miRNA studied was determined based on the  
23 principle of the minimum signal-to-noise ratio of 10, a typical constant used to define the minimum  
24 concentration at which an analyte can be reliably quantified [15]. Therefore, LoQ was calculated as  
25 the Cycle Threshold (Ct) value that is 3.2 Ct units lower than the limit of blank (LoB) (Ct value detected  
26 in non-template controls, i.e., a blank array run with the master mix but without RNA sample). This  
27 difference provides a factor ten times higher in LoQ (assuming a doubling miRNA product per cycle)  
28 and considering that Ct values are inversely proportional to miRNA expression. Samples with Ct higher  
29 than the established LoQ were supposed not to have expressed the analyzed miRNA. Relative changes  
30 in mRNA and miRNA expression were analyzed by multiple T-tests with false discovery rate (FDR)  
31 correction using Benjamini and Hochberg's method. Data were analyzed and plotted using GraphPad  
32 Prism version 10.4 (GraphPad Software, San Diego, CA, USA).

## 34 **Data Availability**

1 Detailed methods related to; 1) extracellular vesicles isolation, characterization, and  
2 quantitation 2) cell culture and EVs treatments; 3) endothelial cell phenotype; 4) miRNA and mRNA  
3 expression and network association; and 5) miRNA-based therapy is described in the Data  
4 Supplement. For a more detailed description of the study population, EVs purification, and  
5 angiogenesis assays, please contact [apvilleladantas@ub.edu](mailto:apvilleladantas@ub.edu).

## 6 7 **Results**

### 8 9 **Patient population**

10 The baseline characteristics of the two groups studied are summarized in **Table 1**, and the  
11 specific clinical characteristics of NSTEMI patients at the time of inclusion are shown in the **Table 2**.  
12 NSTEMI group showed on admission a higher percentage of hypertension and hypercholesterolemia,  
13 but similar body mass index and proportion of smoker individuals than the control group. No  
14 differences were found in the frequency distribution by age and sex.

### 15 16 **Characterization and quantification of EVs**

17 Purification of EVs from plasma using a combination of precipitation and size exclusion  
18 chromatography (SEC) resulted in a population of nanoparticles with a mean size distribution of 73  
19 nm (95%; CI: 65–80 nm) when considering all samples from both groups (**Figure 1A**). There were no  
20 differences in the size distribution of nanoparticles isolated from controls in comparison to those  
21 purified from NSTEMI patients (**Figure 1B**). When the concentration of EVs was determined by  
22 acetylcholinesterase activity, a known exosomal enzyme, samples from NSTEMI patients showed a  
23 higher concentration of EVs per mL of plasma than those of control subjects (**Figure 1C**). Semi-  
24 quantitative exo-check antibody array demonstrated the presence of EV protein markers in EVs from  
25 both groups (**Supplementary Figure I**). Distribution of CD9, CD63 and CD81 markers in SEC fractions  
26 were similar in EVs from control and NSTEMI groups (**Supplementary Figure I**).

### 27 28 **Effects of circulating EVs on ECs function**

29 After 48 h of incubation with EVs, the angiogenic potential of ECs (HUVEC) and the  
30 development of morphological vascular characteristics were estimated based on their migratory rate,  
31 their ability to form tube-like structures (angiogenesis) and to disperse as long branches and  
32 anastomoses throughout a matrix (vascular morphogenesis). As shown in **Figure 2**, EVs treatment  
33 significantly increased the migratory rate of HUVECs when compared to Sham-treated cells.  
34 Nevertheless, although migration was increased in both groups of HUVEC treated with EVs, there was

1 no differences when comparing the migration rate in ECs treated with EVs purified from Control and  
2 NSTEMI (**Figure 2**).

3 We next used two well-established *in vitro* assays to evaluate endothelial tip cell formation  
4 and endothelial stalk elongation at early stages of branching (Matrigel™ tube formation assay) and EC  
5 behavior in vascular morphogenesis (3D angiogenesis in fibrin gel). With these assays, we found that  
6 treatment with EVs from control subjects increased the number of sprouts junctions, segments and  
7 the tube-like structures (meshes) by ECs (**Figure 3A and Figure 3B**). In contrast, when HUVEC were  
8 treated with EVs from NSTEMI patients they exhibited an equivalent angiogenic potential as Sham-  
9 treated cells. Moreover, several samples in the NSTEMI group showed a random proliferative profile  
10 in the Matrigel (**Figure 3A, white arrow in photomicrograph**).

11 To further understand the role of EVs in vessel formation, vascular morphogenesis was  
12 determined by measuring the number of sprout tips and the distance of the cell elongations to the  
13 center of the bead. In this protocol, we observed two different types of cellular behavior concerning  
14 matrix invasion. In some samples, ECs detached from the beads and proliferated with a random walk  
15 and few sprouts (<3 sprout elongations per bead), which we classified as a proliferative profile. In  
16 other samples, ECs detached from the beads as numerous and long sprouts, forming a vessel-like  
17 structure with branches and anastomosis, named as sprouting profile (**Figure 3C, representative**  
18 **images as indicated**). The frequency of sprouting profile was markedly higher in ECs treated with EVs  
19 from control subjects ( $p = 0.032$ ) in comparison to Sham-treated or cells treated with EVs from NSTEMI  
20 patients (**Figure 3D**). As a result, a higher number of sprouting/bead with longer branches was  
21 observed in the control group (**Figure 3E**). Those results suggest, that EVs from NSTEMI inhibit the  
22 angiogenic potential of ECs despite their increased migratory rate.

### 24 **Mechanisms involved in EV-driven modulation of ECs angiogenic potential**

25 We next sought to determine the mechanism by which the different groups of EVs modulate  
26 ECs phenotype to activate or hamper their potential to form new vessels. In this regard, we first  
27 assessed the angiogenic protein profiles of the EVs from NSTEMI patients and control volunteers using  
28 antibody arrays and compared for their pro- and antiangiogenic features (**Supplementary Figure II**).  
29 Of the proteins detected by these arrays, we observed changes in the expression of pro- and  
30 antiangiogenic proteins in EVs of NSTEMI group compared to control ones. Of the three antiangiogenic  
31 proteins highly expressed in EVs, we observed differences in both directions. While PF4 expression  
32 was higher in EVs from control volunteers, TSP-1 protein was markedly lower in EVs from NSTEMI.  
33 PEDF expression was similar in both groups (**Supplementary Figure II**). On the other hand, of the pro-  
34 angiogenic proteins expressed in EVs, we observed that the levels of ANG, IGFBP-3, and MMP-9 were

1 markedly higher in control EVs compared to NSTEMI (**Supplementary Figure II**). The protein PAI-1 with  
2 dual effect was also more expressed in EVs of control than NSTEMI (**Supplementary Figure II**).

3 We also performed an analysis gene expression profile after 48 h of treatment with EVs using  
4 two gene expression panels based on quantitative real-time PCR to amplify 178 genes involved in  
5 angiogenesis and vascular morphogenesis. The **Supplementary Table I** shows the information of genes  
6 studied with their respective values of fold change in reference to Sham-treated expression and p-  
7 value from univariate analysis and q-values after FDR correction. Genes that were significantly  
8 modified in HUVEC treated with EVs from both controls and NSTEMI groups (q-value < 0.05) were  
9 clustered, using an autosome attribute algorithm, into a heatmap representation according to their  
10 similarity in the pattern of expression across samples (**Figure 4A**). Of the 178 genes analyzed, we found  
11 that 34 mRNA expression were modified in the control group; most of them (29 genes) were up-  
12 regulated (**Figure 4B**). In opposition to the NSTEMI group, EV treatment induced the downregulation  
13 of 52 genes (**Figure 4C**); most of them showed opposite expression patterns than that seen in the  
14 control group (**Supplementary Table I**).

15 The miRNAs represent an important part of EVs cargo and are major players in the regulation  
16 of intercellular communication and signaling. Differences in miRNA profile in circulating EVs of NSTEMI  
17 patients were determined by miRNA array and were expressed as fold change (Log<sub>2</sub>) in reference to  
18 the expression in circulating EVs from control subjects (**Supplementary Table II**). With this analysis,  
19 we could observe a differential expression of 10 miRNAs (**Figure 4D**), being four of them up-regulated  
20 in NSTEMI [hsa-miR-125a-5p; hsa-miR-199a-3p; hsa-miR-208b-3p; hsa-miR-499a-5p], and the other  
21 six miRNAs decreased in those patients [hsa-let-7b-5p; hsa-miR-1249-3p; hsa-miR-142-3p; hsa-miR-  
22 190a-5p; hsa-miR-374a-3p; hsa-miR-671-3p] (**Figure 4E**).

23 miRNAs can modify cellular phenotype by post-transcriptional modulation of gene expression  
24 regulation through either the degradation of a transcript or the inhibition of translation [16]. We used  
25 miRnet database to create a network of validated miRNA-mRNA interaction for better visualization of  
26 how miRNA differentially expressed in EVs of NSTEMI could correlate with changes in mRNA  
27 expression in HUVEC (**Figure 4F**). We found three miRNAs modified in NSTEMI EVs that are associated  
28 with downregulation of major components of vasculogenic process: miR-199a-3p, let-7b-5p, and miR-  
29 125a-5p (**Figure 4F**). The downregulation of let-7b-5p typically promotes angiogenesis, as let-7b-5p is  
30 known to suppress pro-angiogenic factors [17]. Therefore, its downregulation in NSTEMI EVs could  
31 not explain the antiangiogenic effect observed. In this regard, we proceeded with the validation of the  
32 two miRNAs whose increase could justify the decreased mRNA expression observed: miR-199a-3p,  
33 and miR-125a-5p. We found that treatment with miR-125a-5p did not modify ECs vasculogenic  
34 potential, while miR-199a-3p slightly decreased sprout number and length (**Figure 5A and 5B**).

1 However, the combination of miR-125a-5p and miR-199a-3p markedly decreased sprout formation  
2 and length (**Figure 5A and 5B**). When EVs from NSTEMI patients were administered in ECs  
3 concomitantly with anti-miRNA therapy, we found that the combination of anti-miR-125a-5p and anti-  
4 miR-199a-3p was able to block the negative effect of these EVs on vasculogenesis (**Figure 5A and 5B**),  
5 establishing the role of miR-125a-5p and anti-miR-199a-3p in the impaired  
6 angiogenesis/vasculogenesis in those patients. mRNA array of genes involved in angiogenesis  
7 regulation showed that a total of 8 genes were downregulated in HUVEC transfected with miR-125a-  
8 5p and anti-miR-199a-3p combo (**Figure 5C**). Of the 178 genes analyzed, we found a downregulation  
9 of major regulators of angiogenesis initiation - VEGF (VEGF, FLT1) and angiopoietin (ANGPT1)  
10 pathways, as well as main transcription regulators of those genes (SMAD3 and STAT3). Moreover, miR-  
11 125a-5p and anti-miR-199a-3p transfection markedly decreased the expression of components that  
12 are crucial for neovessel stability, such as COL4A2, COL4A5 and CDH5. A second network was  
13 constructed combining the miRnet database and the Gene Ontology pathways for better visualization  
14 and integration of miRNAs, genes and pathways (**Figure 5D**).

15

## 16 **Discussion**

17 Our study demonstrates that circulating EVs play a crucial role in modulating the signaling of  
18 ECs, thereby influencing their angiogenic behavior. However, the EVs released into the circulation  
19 during an AMI exhibit a distinct profile in molecular cargo compared to those from healthy individuals.  
20 This difference alters the phenotype of endothelial cells, affecting their angiogenic potential. While  
21 EVs from healthy donors demonstrate a strong pro-angiogenic effect on ECs, enhancing in vitro cell  
22 migration and promoting the formation of microvessel-like structures, the EVs released following  
23 NSTEMI lack this vital pro-angiogenic capability, highlighting a critical shift in vascular response during  
24 acute myocardial events. Network analysis of the miRNA content within the EVs, along with observed  
25 changes in mRNA expression in ECs treated with these vesicles and miR-based therapy, indicates that  
26 the antiangiogenic signaling associated with NSTEMI EVs is primarily mediated by elevated levels of  
27 miR-199a-3p and miR-125a-5p.

28 The contribution of endogenous EVs to angiogenesis has been amply demonstrated by  
29 experimental studies and associated with clinical conditions, mostly centered on cancer research [18].  
30 However, although the use of EVs derived from specific conditioned cells has raised many promises in  
31 the field of cardiac regeneration [19-21], we are still walking in the dark when it comes to the  
32 contribution of endogenous EVs to the cardiovascular pathophysiology. The involvement of  
33 endogenous EVs to neovascularization in the heart, and more specifically during the ischemic process,  
34 is still poorly understood. In this context, we began to decrypt the role and underlying mechanisms of

1 circulating EVs in the pathophysiology of AMI by determining their action at a critical aspect in the  
2 pathophysiology of CVD, the process of neovascularization.

3 During AMI, oxygen and inflammatory sensors in cells can trigger the activation and release  
4 of EVs, which may function in both autocrine and paracrine manners to promote the formation of new  
5 blood vessels [22]. In this study, we observed a higher concentration of EVs in the plasma of patients  
6 during an acute NSTEMI event in comparison to control subjects. This elevation likely reflects a  
7 detrimental apoptotic environment within the heart, as well as a response from the ischemic and  
8 inflamed myocardium attempt at enhancing tissue perfusion. Yet, despite this substantial release of  
9 circulating EVs during the cardiac ischemic event, our findings reveal that these EVs do not effectively  
10 foster new blood vessel formation. Endothelial cells treated with EVs from NSTEMI patients  
11 demonstrated a marked reduction in angiogenic capacity, suggesting that the angiogenic responses  
12 by EVs are more closely related to the specific molecular cargo contained within these vesicles rather  
13 than their overall abundance in circulation. Considering the variety of stimuli and cell population  
14 activated during AMI, it is crucial to bear in mind that we are facing an extremely heterogeneous  
15 population of EVs from a diverse population of activated cells that may be sending disparate  
16 intercellular signals to either stimulate or prevent angiogenesis. Moreover, the diversity within EVs  
17 molecular cargo in the same cell population can be influenced by a range of factors influencing their  
18 biogenesis process. It is proposed that this finely tuned cargo-loading mechanism enables cells to  
19 selectively eliminate unnecessary or excess materials that may result from various metabolic  
20 activities, cellular stress responses, or disruptions in homeostasis [23]. For that reason, we can assume  
21 that responses triggered by circulating EVs in AMI can be influenced not only by the number of EVs  
22 being released but also by the differential molecular cargo they contain depending on the donor cell  
23 type or the stimulus for their release.

24 Within the molecular cargo in the EVs, miRNA package represents one of the foremost  
25 regulators of cellular phenotype, which in most cases, negatively regulate the expression of protein-  
26 coding genes by promoting degradation or suppressing translation of target mRNAs [24]. In this  
27 regard, the substantial downregulation of pro-angiogenic genes observed in ECs of NSTEMI group  
28 could be a result of clustered degradation of those mRNA by specific combo of miRNAs in EVs. An  
29 array of miRNA expression revealed a group of ten miRNA of more than 700 sequences analyzed that  
30 were differentially expressed in EVs of NSTEMI. The interaction of those miRNA with genes modified  
31 in the NSTEMI group was spot in a network for visualization and integration of miRNAs, genes, and  
32 pathways. The network, built based on the mRNAs that had low expression in the NSTEMI group using  
33 the ten modified miRNAs as the target hub, shows the integration of fourteen negatively regulated  
34 mRNAs in ECs by five miRNAs expressed in the NSTEMI EVs. Nonetheless, only two of these candidates

1 were up-regulated in NSTEMI EVs and could be associated with the lower regulation of genes  
2 observed, miR-125a-5p and mir-199a-3p.

3 Emerging research has highlighted the significant roles of miR-125a-5p and miR-199a-3p in  
4 influencing AMI outcomes. Current findings suggest that miR-125a-5p and miR-199a-3p can offer  
5 protective benefits to the heart following AMI; however, its impact on cardiovascular health may vary  
6 significantly depending on the context. A recent study by Gao et al. (2023) reported that miR-125a-5p  
7 delivered via exosomes derived from mesenchymal stem cells, significantly enhanced cardiac repair  
8 in mouse models of myocardial ischemia/reperfusion. This intervention was associated with  
9 substantial improvements in cardiac function, reduced adverse remodeling, angiogenesis and a  
10 favorable shift in macrophage polarization toward an anti-inflammatory phenotype [25]. In contrast,  
11 research found that miR-125a-5p was upregulated in the peripheral blood mononuclear cells of post-  
12 AMI patients and was associated with left ventricular systolic dysfunction, a common contributor to  
13 heart failure [26]. When examining angiogenesis, miR-125a-5p also exhibits a complex profile,  
14 demonstrating both pro- and antiangiogenic effects that may depend on the specific cellular and  
15 pathophysiologic context. Specifically, in conditions associated with AMI, such as senescence [27] and  
16 inflammation [28], miR-125a-5p predominantly shows antiangiogenic properties by directly targeting  
17 pro-angiogenic genes, such as VEGF and eNOS [27].

18 The role of miR-199a-3p in the infarcted heart has also been reported shown, although  
19 conflicting data in the literature are found. Patients with elevated serum levels of miR-199a had a  
20 positive correlation with troponin levels, a negative correlation with left ventricular ejection fraction,  
21 and a higher likelihood of experiencing major adverse cardiac event [29]. On the other hand, basic  
22 science studies have associated this miRNA with cardiac repair following ischemic injury. Exogenous  
23 miR-199a-3p administration can increase cardiomyocyte proliferation in (human hybrid and primary  
24 mouse) cell lines [30], and local miR-199a-3p delivery can improve heart function and mice survival  
25 after AMI [31]. Regarding blood vessel formation, miR-199a-3p can also influence the expression of  
26 angiogenic factors and pathways, thereby potentially affecting the formation of new blood vessels  
27 [32]. However, the specific mechanisms and targets involved in this process are still under  
28 investigation.

29 In our study, transfection of ECs with individual mimics of miR-125a-5p and miR-199a-3p  
30 caused minor effects on their angiogenic capacity. However, the combination of both miRNA (miR-  
31 125a-5p + mir-199a-3p) markedly decreased sprout number and length in the 3D model of  
32 vasculogenesis. Moreover, treatment of ECs with the combination of anti-miR-125a-5p and anti-miR-  
33 199a-3p was able to block the negative effect of NSTEMI EVs on vasculogenesis, establishing the role

1 of combined increase of miR-125a-5p and miR-199a-3p in the impaired angiogenesis/vasculogenesis  
2 in NSTEMI patients.

3         The onset of angiogenesis and EC fate during this process is a complex multistep event  
4 regulated by the fine-tuning of molecules involved in cell sprouting, migration, proliferation, and  
5 survival (Reviewed in references [33-36]). Understanding the molecular mechanisms underlying  
6 these processes is vital for elucidating the role of circulating EVs in the pathophysiology of AMI. In  
7 our analysis of a range of mRNAs encoding key players in angiogenesis and vascular remodeling, we  
8 observed that treatment with EVs alters the expression of many of these components in the  
9 endothelial cells. Notably, these changes were often opposite in direction between the control and  
10 NSTEMI groups. Specifically, when treating endothelial cells with EVs from NSTEMI patients or with a  
11 combination of miR-125a-5p and miR-199a-3p, we saw a significant decrease in the mRNA  
12 expression of critical components involved in blood vessel formation. Most significantly, we found  
13 downregulation of crucial elements within two fundamental pathways that are vital for the  
14 transition and maintenance of the EC phenotype during vessel formation: 1) the vascular endothelial  
15 growth factor (VEGF, FLT1); and 2) the Angiopoietin (AngPT1) signaling pathways. Moreover, EC  
16 treatments with EVs and miR-125a-5p+miR-199a-3p combo reduced the mRNA expression of the  
17 transcription regulators SMAD3 and STAT3. Activation of STAT 3 and SMAD3 has been associated  
18 with the upregulation of anti-apoptotic and pro-angiogenic genes, including VEGF, contributing to  
19 improved cardiac function and repair mechanisms post-MI [37, 38].

20         Interestingly, we found that the treatment with NSTEMI extracellular vesicles (EVs) and a  
21 combination of miRNAs also leads to a downregulation of collagen IV subunits in endothelial cells  
22 (ECs). This effect could, paradoxically, promote the onset of angiogenesis rather than inhibit it.  
23 However, it is essential to highlight that while the degradation of collagen IV is a vital initial step in  
24 promoting the sprouting of ECs, a rapid turnover of collagen IV also plays a pivotal role in ensuring the  
25 stability and structural integrity of the newly developed vascular network [39]. Thus, a sustained  
26 decrease in collagen IV expression poses a risk of compromising both the stability and the overall  
27 morphology of the neovasculature, potentially leading to impaired function of the newly formed blood  
28 vessels.

29         In summary, this study demonstrates the neovasculogenic potential of circulating EVs of  
30 healthy individuals, based on their ability to boost EC sprouting via activation of pathways associated  
31 with matrix reorganization, phenotype shuffling and network stability. In contrast, the molecular  
32 profile of circulating EVs during acute NSTEMI events lack their angiogenic potential as their  
33 incorporation into ECs reduces sprouting and morphogenesis, via downregulation of several pro-  
34 angiogenic pathways. An increase in the expression or packing of miR-125a-5p and miR-199a-3p in

1 the EVs of NSTEMI can partially contribute to the impaired EC function and may represent a hazard in  
2 the pathophysiology and outcome of AMI.

3

#### 4 **Translational Perspective**

5 EVs released into the circulation in acute coronary syndrome may exhibit specific profile of  
6 miRNAs or other cargos that could provide valuable information on disease progression and predict  
7 patient outcome. Combining this feature with their stability in body fluids turn EVs into a useful source  
8 of diagnosis and prognostic biomarker in CVD. Moreover, EVs of healthy individuals display a great  
9 angiogenic potential that could be exploited for cardiac regeneration. Identifying the pro-angiogenic  
10 cargo in the healthy EVs will eventually allow the tailoring of nanovesicles with specific profile  
11 targeting to improve neovascularization in the infarcted myocardium.

12

#### 13 **Study limitations**

14 Although our data provides novel and valuable insights into the complexity of EVs' role in CVD,  
15 we are aware of the limitations of this study, many of which are still unknown variables in this field.  
16 For instance, it was not possible in the present study to specify the cellular source of circulating EVs,  
17 since our protocol isolated small EVs by size exclusion and not using specific cell membrane markers.  
18 Therefore, defining the origin and conditions that regulate the release of a specific profile of EVs in  
19 the heart remains a major yet challenging task. We are aware of the importance of this information,  
20 and we are currently working in complex studies with more specific protocols to identify the cellular  
21 source of EVs and separate their specific contribution to NSTEMI pathophysiology. Furthermore, in  
22 this study, we count with a significantly low number of women, as a reflex of lower incidence of  
23 women with NSTEMI in our hospital. We recognize the existing gender gap in cardiovascular research  
24 and the significant need to investigate how sex influences cardiovascular pathophysiology, as well as  
25 potential biomarkers such as miRNAs and EVs cargo. Therefore, upcoming studies involving a larger  
26 cohort, must prioritize the inclusion of women with AMI to ensure equitable representation of both  
27 sexes in EVs research. Moreover, we are unable to determine whether the antiangiogenic EVs in  
28 NSTEMI patients could be predictive of AMI risk (because patient's low capacity to form collaterals),  
29 or if they could be used in the prognosis of poor outcome after AMI. It is important to note that, in  
30 our study, not all NSTEMI patients had circulating EVs with antiangiogenic profile. There was still a  
31 small percentage (25%) of patients in which their EVs showed good angiogenic potential despite  
32 having suffered an AIM event. The difference in responses in NSTEMI group despite sharing similar  
33 clinical conditions could represent a differential regulation in the pathophysiology of AMI. Regrettably,  
34 the size of our cohort and the time point in our study do not provide sufficient statistical power to

1 allow any assumption in the correlation between EV profile and patient outcome, or to determine sex-  
2 associated differences in miRNA profile. Our results, however, shed much light on this topic by  
3 showing that circulating EVs have a specific fingerprint that can be associated with the onset and  
4 progression of coronary disease. The predictive or therapeutic potential of these nanovesicles must  
5 be analyzed by our group, and by others, in a larger cohort with more clinical information on cardiac  
6 perfusion.

7

#### 8 **Authors' Contributions**

9 All authors have substantially contributed to the conception, design, and interpretation of the study  
10 (Dantas, Brugaletta, Fernandez-Bacerra); patient inclusion, sample acquisition, data interpretation  
11 and outcome analysis (Brugaletta, Sabate, Ortega-Paz, Rodriguez, García-Alvarez); execution of  
12 experimental protocol and data analysis (Dantas, Bobi, Jimenez-Trinidad, Cortes-Serra and Lazaro).

13

#### 14 **Acknowledgments**

15 We are grateful to the nurses of the ICCV, Anna Barrabes and Elisabet De Mingo for their careful and  
16 efficient work with blood sampling. We also thank the Genomic Core at IDIBAPS for RNA analysis with  
17 Bioanalyzer, and the "Soft-Materials" core facility at the Institute of Material Science of Barcelona,  
18 Superior Council of Scientific Research (CSIC) for analysis of nanoparticles with nanosight.

19

#### 20 **Source of Funding**

21 This work was supported by Spanish funds from Ministerio de Economía y Competitividad, Instituto  
22 de Salud Carlos III - FEDER-ERDF (PI16/00742, PI19/00264); and the Spanish Society of Cardiology  
23 (SEC/FECINV- BAS 20/012). IDIBAPS belongs to the CERCA Programme and receives partial funding  
24 from the Generalitat de Catalunya and cofunding provided by the Fondo Europeo de Desarrollo  
25 Regional (FEDER). Research on extracellular vesicles in the laboratories of CF-B is funded by grants  
26 from the Spanish Ministry of Science and Innovation (MICINN) (PID2022-142908OB-I00) and co-  
27 financed by AGAUR-SGR (2021 SGR 01554). We also acknowledge support from the grant CEX2023-  
28 0001290-S funded by MCIN/AEI, and support from the Generalitat de Catalunya through the CERCA  
29 Program. CFB is also part of the CIBER-Consorcio Centro de Investigación Biomédica en Red (CB 2021),  
30 Instituto de Salud Carlos III, Ministerio de Ciencia e Innovación, and Unión Europea-  
31 NextGenerationEU.

32

#### 33 **Disclosures**

34 The authors declare no competing interests.

1  
2  
3  
4  
5  
6  
7  
8  
9  
10  
11  
12  
13  
14  
15  
16  
17  
18  
19  
20  
21  
22  
23  
24  
25  
26  
27  
28  
29  
30  
31  
32  
33  
34  
35

## Supplemental Material

Supplemental material includes: 1) Expanded Materials & Methods; 2) Supplementary Figures I-III; 3) Supplementary Tables I-II.

## References

1. Alberts B, J.A., Lewis J, *General Principles of Cell Communication*, in *Molecular Biology of the Cell*. 2002, Garland Science. p. 1464.
2. van Niel, G., G. D'Angelo, and G. Raposo, *Shedding light on the cell biology of extracellular vesicles*. *Nat Rev Mol Cell Biol*, 2018. **19**(4): p. 213-228.
3. Boulanger, C.M., et al., *Extracellular vesicles in coronary artery disease*. *Nat Rev Cardiol*, 2017. **14**(5): p. 259-272.
4. Kablak-Ziembicka, A., R. Badacz, and T. Przewlocki, *Clinical Application of Serum microRNAs in Atherosclerotic Coronary Artery Disease*. *J Clin Med*, 2022. **11**(22).
5. Kablak-Ziembicka, A., et al., *Cardiac microRNAs: diagnostic and therapeutic potential*. *Arch Med Sci*, 2023. **19**(5): p. 1360-1381.
6. Baruah, J. and K.K. Wary, *Exosomes in the Regulation of Vascular Endothelial Cell Regeneration*. *Front Cell Dev Biol*, 2019. **7**: p. 353.
7. Koerselman, J., et al., *Coronary collaterals: an important and underexposed aspect of coronary artery disease*. *Circulation*, 2003. **107**(19): p. 2507-11.
8. Potz, B.A., et al., *Novel molecular targets for coronary angiogenesis and ischemic heart disease*. *Coron Artery Dis*, 2017. **28**(7): p. 605-613.
9. de Menezes-Neto, A., et al., *Size-exclusion chromatography as a stand-alone methodology identifies novel markers in mass spectrometry analyses of plasma-derived vesicles from healthy individuals*. *J Extracell Vesicles*, 2015. **4**: p. 27378.
10. Ciudad, P., et al., *K<sup>+</sup> channels expression in hypertension after arterial injury, and effect of selective Kv1.3 blockade with PAP-1 on intimal hyperplasia formation*. *Cardiovasc Drugs Ther*, 2014. **28**(6): p. 501-11.
11. Mompeon, A., et al., *Circulating miRNA Fingerprint and Endothelial Function in Myocardial Infarction: Comparison at Acute Event and One-Year Follow-Up*. *Cells*, 2022. **11**(11).
12. Nakatsu, M.N. and C.C. Hughes, *An optimized three-dimensional in vitro model for the analysis of angiogenesis*. *Methods Enzymol*, 2008. **443**: p. 65-82.
13. Fan, Y., et al., *miRNet - dissecting miRNA-target interactions and functional associations through network-based visual analysis*. *Nucleic Acids Res*, 2016. **44**(W1): p. W135-41.

- 1 14. Kadam, P. and S. Bhalerao, *Sample size calculation*. Int J Ayurveda Res, 2010. **1**(1): p. 55-7.
- 2 15. Wolfinger, R.D., et al., *Two approaches for estimating the lower limit of quantitation (LLOQ) of*  
3 *microRNA levels assayed as exploratory biomarkers by RT-qPCR*. BMC Biotechnol, 2018. **18**(1): p.  
4 6.
- 5 16. Ambros, V., *The functions of animal microRNAs*. Nature, 2004. **431**(7006): p. 350-5.
- 6 17. Henn, D., et al., *MicroRNA-regulated pathways of flow-stimulated angiogenesis and vascular*  
7 *remodeling in vivo*. J Transl Med, 2019. **17**(1): p. 22.
- 8 18. Hessvik, N.P. and A. Llorente, *Current knowledge on exosome biogenesis and release*. Cell Mol  
9 Life Sci, 2018. **75**(2): p. 193-208.
- 10 19. Potz, B.A., et al., *Extracellular Vesicle Injection Improves Myocardial Function and Increases*  
11 *Angiogenesis in a Swine Model of Chronic Ischemia*. J Am Heart Assoc, 2018. **7**(12).
- 12 20. Roefs, M.T., et al., *Cardiac progenitor cell-derived extracellular vesicles promote angiogenesis*  
13 *through both associated- and co-isolated proteins*. Commun Biol, 2023. **6**(1): p. 800.
- 14 21. Li, Q., et al., *Small extracellular vesicles containing miR-486-5p promote angiogenesis after*  
15 *myocardial infarction in mice and nonhuman primates*. Sci Transl Med, 2021. **13**(584).
- 16 22. Chistiakov, D.A., A.N. Orekhov, and Y.V. Bobryshev, *Cardiac Extracellular Vesicles in Normal and*  
17 *Infarcted Heart*. Int J Mol Sci, 2016. **17**(1).
- 18 23. Gurunathan, S., et al., *Biogenesis, Membrane Trafficking, Functions, and Next Generation*  
19 *Nanotherapeutics Medicine of Extracellular Vesicles*. Int J Nanomedicine, 2021. **16**: p. 3357-3383.
- 20 24. Emanuelli, C., et al., *Exosomes and exosomal miRNAs in cardiovascular protection and repair*.  
21 Vascul Pharmacol, 2015. **71**: p. 24-30.
- 22 25. Gao, L., et al., *Therapeutic delivery of microRNA-125a-5p oligonucleotides improves recovery*  
23 *from myocardial ischemia/reperfusion injury in mice and swine*. Theranostics, 2023. **13**(2): p.  
24 685-703.
- 25 26. Dantas-Komatsu, R.C.S., et al., *The let-7b-5p, miR-326, and miR-125a-3p are associated with left*  
26 *ventricular systolic dysfunction in post-myocardial infarction*. Front Cardiovasc Med, 2023. **10**: p.  
27 1151855.
- 28 27. Che, P., et al., *miR-125a-5p impairs endothelial cell angiogenesis in aging mice via RTEF-1*  
29 *downregulation*. Aging Cell, 2014. **13**(5): p. 926-34.
- 30 28. Wade, S.M., et al., *Dysregulated miR-125a promotes angiogenesis through enhanced glycolysis*.  
31 EBioMedicine, 2019. **47**: p. 402-413.
- 32 29. Xu, L., et al., *The diagnostic and prognostic value of serum miR-199a-5p combined with*  
33 *echocardiography in acute myocardial infarction*. J Cardiothorac Surg, 2025. **20**(1): p. 42.

- 1 30. Wang, X.Z., et al., *MiR-199a-3p promotes repair of myocardial infarction by targeting NACC2*. Int  
2 J Clin Exp Pathol, 2023. **16**(3): p. 57-66.
- 3 31. Lesizza, P., et al., *Single-Dose Intracardiac Injection of Pro-Regenerative MicroRNAs Improves*  
4 *Cardiac Function After Myocardial Infarction*. Circ Res, 2017. **120**(8): p. 1298-1304.
- 5 32. Joris, V., et al., *MicroRNA-199a-3p and MicroRNA-199a-5p Take Part to a Redundant Network of*  
6 *Regulation of the NOS (NO Synthase)/NO Pathway in the Endothelium*. Arterioscler Thromb Vasc  
7 Biol, 2018. **38**(10): p. 2345-2357.
- 8 33. Potente, M., H. Gerhardt, and P. Carmeliet, *Basic and therapeutic aspects of angiogenesis*. Cell,  
9 2011. **146**(6): p. 873-87.
- 10 34. Chen, W., et al., *The endothelial tip-stalk cell selection and shuffling during angiogenesis*. J Cell  
11 Commun Signal, 2019. **13**(3): p. 291-301.
- 12 35. De Smet, F., et al., *Mechanisms of vessel branching: filopodia on endothelial tip cells lead the*  
13 *way*. Arterioscler Thromb Vasc Biol, 2009. **29**(5): p. 639-49.
- 14 36. Herbert, S.P. and D.Y. Stainier, *Molecular control of endothelial cell behaviour during blood*  
15 *vessel morphogenesis*. Nat Rev Mol Cell Biol, 2011. **12**(9): p. 551-64.
- 16 37. Martin-Bornez, M., et al., *New Insights into the Reparative Angiogenesis after Myocardial*  
17 *Infarction*. Int J Mol Sci, 2023. **24**(15).
- 18 38. Bujak, M., et al., *Essential role of Smad3 in infarct healing and in the pathogenesis of cardiac*  
19 *remodeling*. Circulation, 2007. **116**(19): p. 2127-38.
- 20 39. Bahramsoltani, M., et al., *Angiogenesis and collagen type IV expression in different endothelial*  
21 *cell culture systems*. Anat Histol Embryol, 2014. **43**(2): p. 103-15.
- 22

1 **Figures Legend**

2

3 **Figure 1. Extracellular vesicles size distribution and quantitation.** Representative image of EVs  
4 particles captured by nanoparticle tracking analysis NanoSight **(A)** and graphical representation of EVs  
5 amount and size distribution in 1 mL of sample **(B)**. Box and whisker plot shows the mean and  
6 distribution of particle size found in Control (n = 12) and NSTEMI (n = 12) groups **(C)**. Figure **(D)** shows  
7 the frequency distribution of EVs concentration per ml of sample of Control (n = 19) and NSTEMI (n =  
8 33). P values of unpaired T-test with Welch's are expressed on top of each Box and whisker plot group  
9 set. Significance was considered when  $p < 0.05$ .

10

11 **Figure 2. Role of extracellular vesicles in endothelial cell migration.** Migratory rate (% Healing)  
12 following scratch of HUVEC sham-treated and treated for 48h with EVs isolated from control and  
13 NSTEMI patients. Non-linear regression curve **(A)** shows the time course of endothelial cell migration  
14 (% Healing) following EV therapy. Box and whisker plot **(B)** shows the mean and distribution of %  
15 Healing at 24h in Sham (n = 19), Control (n = 19) and NSTEMI (n = 33) groups. The extra sum-of-squares  
16 F determined differences in the fit of time-course curves. Brown Forsythe and Welch ANOVA analyzed  
17 the dependence of data on the type of treatment with Dunnett's T3 post-hoc analysis for multiple  
18 comparisons at 24h after the scratch. P values and comparison are expressed next to the time-course  
19 curve and on top of Box and whisker plot. Significance is considered when  $p < 0.05$ .

20

21 **Figure 3. Role of circulating extracellular vesicles in angiogenesis and vascular morphogenesis.**  
22 Representative photomicrographs show the differential responses of HUVEC to EVs in Matrigel-coated  
23  $\mu$ -Angiogenesis Slides **(A)**. Angiogenesis potential was determined by the number of junctions,  
24 number of segments and number of meshes, as indicated **(B)**. EVs' effect in vascular morphogenesis  
25 was determined by 3D angiogenesis in fibrin gel. When ECs detached from collagen-coated beads,  
26 they exhibited either proliferative (little sprouting and high proliferation and migration) or sprouting  
27 (capillary branches which migrated and invaded fibrin gel) phenotypes **(C)**. Bar graphs **(D)** show the  
28 frequency of each phenotype in Sham- or EV-treated HUVEC. The effects of EVs in vascular  
29 morphogenesis was determined by the ability of ECs to disperse throughout a matrix (sprout number)  
30 and associate into microvessel-like structures (sprout length) **(E)**. Box and whisker plots show the  
31 distribution of the data at different values with respective median (long dash) and quartiles (dotted  
32 line) found in Sham-treated (n = 8), Control (n = 19) and NSTEMI (n = 33) groups. Brown Forsythe and  
33 Welch ANOVA analyzed the dependence of data on the type of EV treatment with Dunnett's T3 post-

1 hoc analysis for multiple comparisons. P values and comparisons are expressed on top of Box and  
2 whisker plot. Significance is considered when  $p < 0.05$ .

3

4 **Figure 4. miRNA expression in circulating extracellular vesicles and interaction with mRNA modified**

5 **by them in HUVEC.** Heatmap of fold change in mRNA expression in pulled HUVEC samples treated

6 with EVs from control (n = 4) or NSTEMI patients (n = 4) **(A)**. Volcano plot of fold change in mRNA

7 expression in HUVEC treated with EVs from Control **(B)** or NSTEMI **(C)** was calculated considering a

8 pull of RNA purified from Sham-treated HUVEC (n = 4) as a reference. The heatmap **(D)** and volcano

9 plot **(E)** of fold change in miRNA expression in each pulled EVs samples from NSTEMI group (n = 10)

10 was calculated considering a pull of miRNA from EVs of control samples (n = 4) as a reference. Volcano

11 plots show the values of fold change (Log<sub>2</sub>, x-axis) by the FDR-adjusted q value (-Log<sub>10</sub> of q-value, y-

12 axis). Highlighted are the genes or miRNAs that were at least 2-fold down-regulated (red) or up-

13 regulated (green). Relative changes in mRNA and miRNA expression were analyzed by multiple T-test

14 with false discovery rate (FDR) correction using the method of Benjamini and Hochberg. Significance

15 is considered when  $q < 0.05$ . The network of interaction of miRNA differentially expressed in EVs of

16 NSTEMI with mRNA modified in HUVEC are shown in figure **(F)**. Circular nodes represent miRNAs that

17 were up-regulated (green) or down-regulated (red) in EVs from NSTEMI which interacts with genes

18 (rectangular nodes) modified in HUVEC after EVs treatment. Size of miRNA nodes are based on their

19 interaction with neighboring mRNA nodes. Edge's length and width reflect betweenness centrality,

20 highlighting (in red) edges that represent the interaction of down-regulated mRNA with up-regulated

21 miRNA in NSTEMI group.

22

23 **Figure 5. miRNA-based therapy in angiogenesis and vascular morphogenesis.** The potential of miR-

24 125a-5p (n = 12), miR-199a-3p (n = 12) and the combination of miR-125a-5p/miR-199a-3p (n = 12) to

25 modulate vascular morphogenesis was determined by the ability of transfected ECs to disperse

26 throughout a matrix [sprout number **(A)**] and associate into microvessel-like structures [sprout length

27 **(B)**]. On the other hand, the potential of anti-miRNA therapy to modify EVs effects were determined

28 by counting sprout number **(A)** and sprout length **(B)** in ECs treated with pulled EVs of NSTEMI patient

29 (n = 10) and transfected with anti-miR-125a-5p (n = 10), anti-miR-199a-3p (n = 10) or the combination

30 of anti-miR-125a-5p/anti-miR-199a-3p (n = 10), as indicated. The association of the miRNA to mRNA-

31 pathways network was based on two miRNAs that had high expression levels in the EVs from NSTEMI

32 patients. Brown Forsythe and Welch ANOVA analyzed the dependence of data on the type of EV

33 treatment with Dunnett's T3 post-hoc analysis for multiple comparisons. Volcano plot of fold change

34 in mRNA expression in HUVEC transfected with a combo of miR-125a-5p and miR-199a mimic **(C)**.

1 Volcano plots show the values of fold change (Log<sub>2</sub>, x-axis) by the FDR-adjusted q value (-Log<sub>10</sub> of q-  
2 value, y-axis). Highlighted are the genes that were at least 2-fold down-regulated (red dots). Relative  
3 changes in mRNA expression were analyzed by multiple T-test with false discovery rate (FDR)  
4 correction using the method of Benjamini and Hochberg. The mRNA-pathway network (**E**) was  
5 constructed based on the consolidated pathways (blue diamond) associated with molecular-level  
6 activities performed by the genes modified in HUVEC treated with EVs from NSTEMI patients (red  
7 circles), FDR < 0.05. P values and comparisons are expressed on top of Box and whisker plot.  
8 Significance is considered when p<0.05.

9  
10 **Graphical Abstract:** This schematic summarizes the experimental workflow and findings on EV-  
11 Mediated Angiogenic Regulation in NSTEMI. **(1)** Plasma samples were collected from NSTEMI  
12 patients (n = 33) and healthy controls (n = 19). The EVs were purified using polymer-based  
13 precipitation (PBP), followed by size-exclusion chromatography (SEC) for molecular weight  
14 fractionation. **(2)** The isolated EVs were analyzed for classical exosome markers CD9, CD63, and  
15 CD81 using flow cytometry and antibody array techniques. Additionally, the size distribution and  
16 concentration of the EVs were determined using nanoparticle tracking analysis. **(3)** Human umbilical  
17 vein endothelial cells (HUVEC) were treated for 48 hours with EVs purified from both control and  
18 NSTEMI patients. **(4)** The functional responses of endothelial cells (ECs) were assessed through cell  
19 migration (using a scratch wound healing assay), 2D angiogenesis (using a tube formation assay), and  
20 3D morphogenesis (using a spheroid sprouting assay). The results showed enhanced angiogenic  
21 responses in ECs treated with control EVs, while NSTEMI-derived EVs reduced both migration and  
22 angiogenesis in the endothelial cells. **(5)** mRNA array analysis revealed changes in pro-angiogenic  
23 and antiangiogenic gene expression in ECs due to EV treatments. EVs from healthy controls led to an  
24 overall upregulation of pro-angiogenic genes, whereas NSTEMI-derived EVs predominantly  
25 downregulated pro-angiogenic genes. **(6)** An array for miRNA profiling identified differentially  
26 expressed miRNAs in NSTEMI versus control EVs. **(7)** An analysis involving miRNA, mRNA, and  
27 functional enrichment suggested that the angiogenesis-related miRNAs, miR-125a-5p and miR-199a-  
28 3p, may contribute to the antiangiogenic effects observed in NSTEMI-derived EVs. **(8)** Validation  
29 studies demonstrated that transfection of a combination of miR-125a-5p and miR-199a-3p  
30 significantly reduced ECs angiogenic capacity. Targeted anti-miRNA therapy, which combinedly  
31 inhibited miR-125a-5p and miR-199a-3p, successfully restored angiogenesis, counteracting the  
32 antiangiogenic effects of NSTEMI EVs.

33

**TABLE 1. Baseline Characteristics**

	<b>Control</b>	<b>NSTEMI</b>	<b>p Value</b>
Age, mean± SD	63.4 ± 7.9	59.8 ± 6.8	0.0690
Sex, n (%)			0.5889
Male	18 (59)	21 (69)	
Female	12 (41)	9 (31)	
BMI, mean± SD	25.4 ± 3.7	27.3 ± 3.8	0.0553
Hypertension, n (%)	3 (10)	25 (84)	<0.0001
Hypercholesterolemia, n (%)	3 (10)	18 (58)	<0.0001
Smoking, n (%)	5 (17)	8 (26)	0.5358

Data are shown as a percentage (%) of frequency or mean ± standard deviation (SD), as indicated. BMI - Body Mass Index; NSTEMI - non-ST-segment elevation myocardial infarction. Continuous variables were compared with unpaired and two-tailed T-test with Welch's correction, and categorical variables were compared with Fisher's exact test.

**TABLE 2. Characteristics of NSTEMI patients at the time of inclusion**

---

Location of coronary lesion, N (%)	
LMC	2 (7)
LAD	19 (63)
Cx	16 (53)
RCA	15 (50)
Creatinine (mg/dl), median [IQR]	1.0 [0.8 – 1.2]
Hemoglobin (g/dl), median [IQR]	13.9 [11.5 – 14.7]
Platelets count, median [IQR]	216 [157 – 264]
Troponin peak (ng/ml), median [IQR]	53 [24 – 133]
Chronic medical treatment before admission, N (%)	
RAS Blocker	24 (80)
Beta Blocker	16 (53)
Statins	17 (57)
Calcium Channel Blocker	20 (14)
Diuretic	14 (47)

---

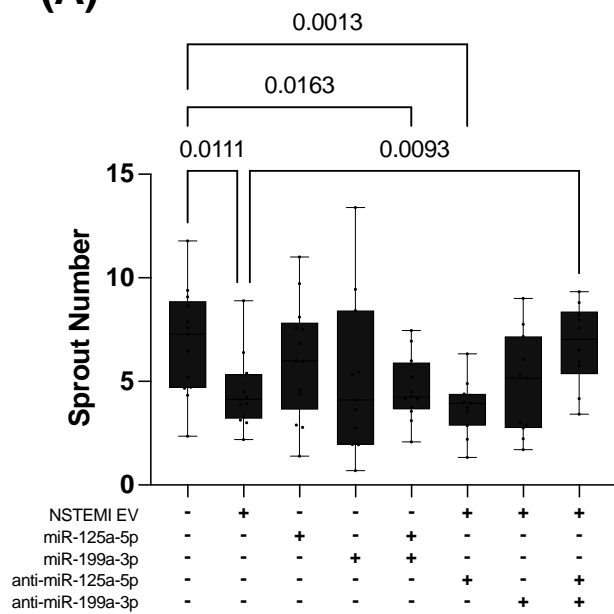
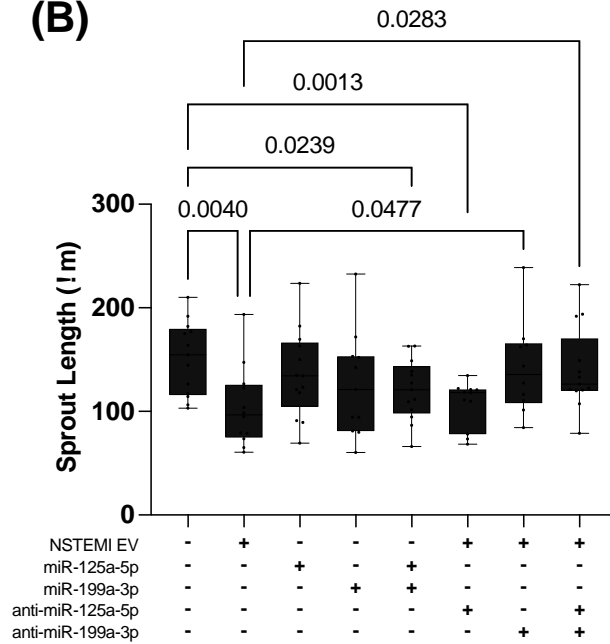
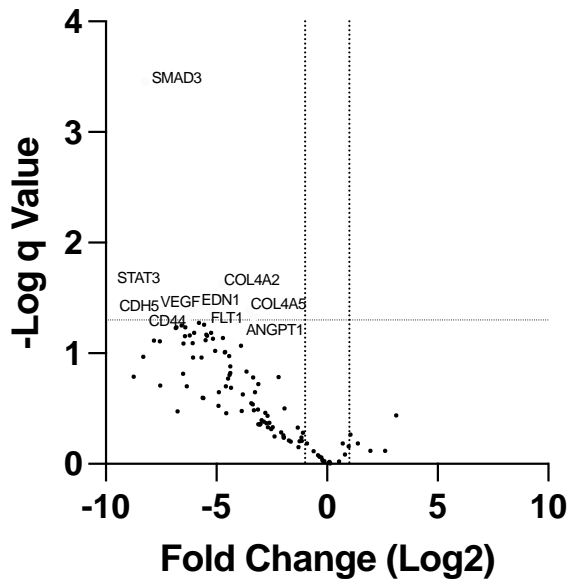
Data are shown as a percentage (%) of frequency or MEDIAN [IQR] as indicated. LMC – Left Main Coronary artery; LAD- Left Anterior Descending artery; Cx - Circumflex artery; RCA - Right Coronary Artery; RAS – Renin-Angiotensin System

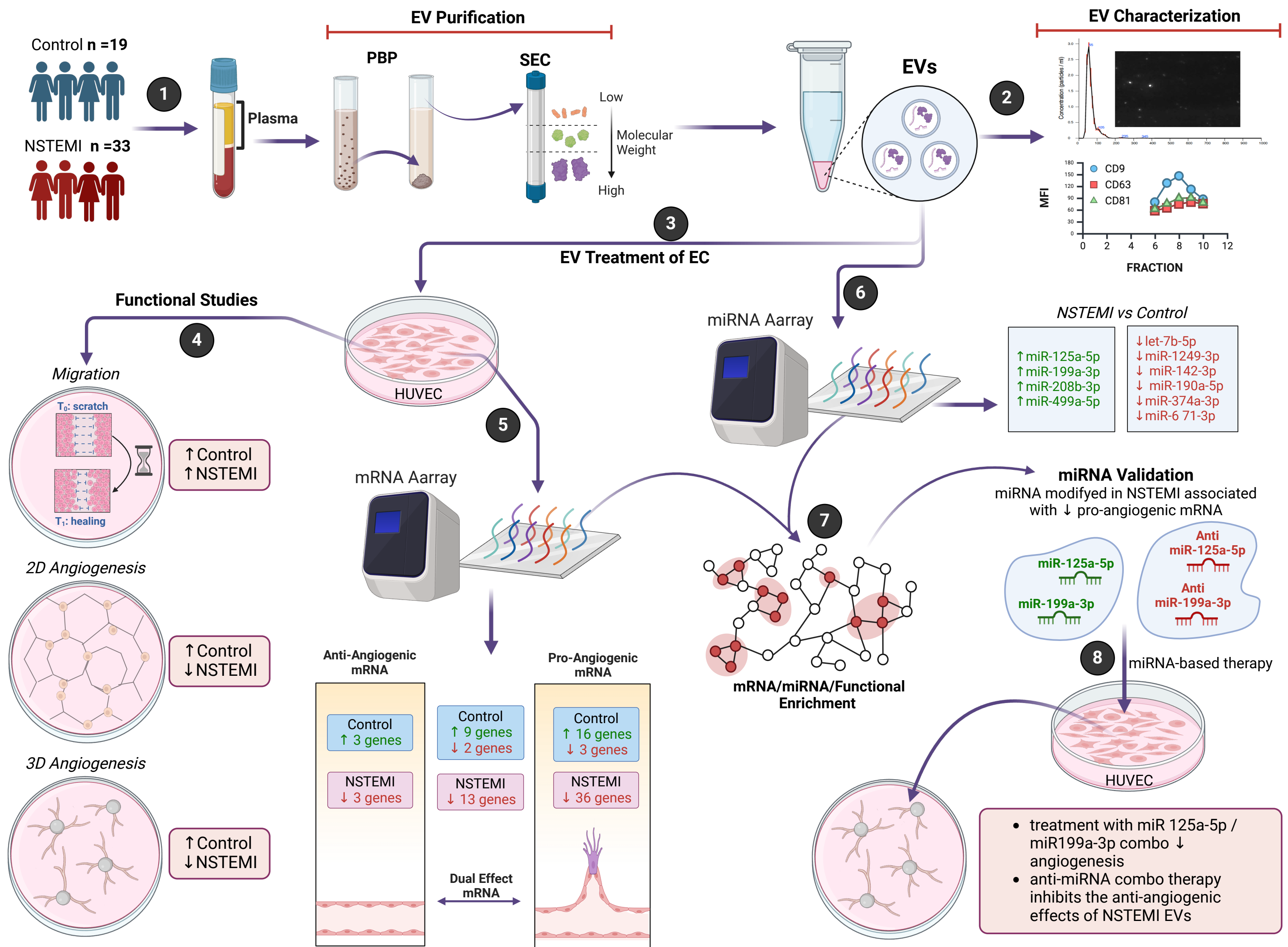








**(A)****(B)****(C)****(D)**



## **Antiangiogenic effect of circulating extracellular vesicles in acute coronary syndrome: role of miR-199a-3p and miR-125a-5p**

**Short Title:** Circulating EVs and angiogenesis in ACS

Joaquin Bobi<sup>1,2</sup>, Francisco-Rafael Jimenez-Trinidad<sup>1,3</sup>, Luis Ortega-Paz<sup>1,2</sup>, Nuria Cortes-Serra<sup>5,6</sup>, Iolanda Lazaro<sup>1</sup>, Juan-Jose Rodriguez<sup>2</sup>, Carmen Fernandez-Becerra<sup>5,6,7</sup>, Ana García-Álvarez<sup>1,2,4</sup>, Manel Sabate<sup>1,2</sup>, Salvatore Brugaletta<sup>1,2</sup>, Ana-Paula Dantas<sup>1,2,3</sup>.

1. Institute of Biomedical Research August Pi Sunyer (IDIBAPS), Barcelona, Spain
2. Institut Clínic Cardiovascular (ICCV), Hospital Clínic, Barcelona, Spain.
3. Department of Biomedicine, School of Medicine and Health Sciences, University of Barcelona, Spain
4. Centro Nacional de Investigaciones Cardiovasculares, Madrid, Spain.
5. ISGlobal, Barcelona Institute for Global Health, Facultat de Medicina i Ciències de la Salut, Universitat de Barcelona (UB), Barcelona, Spain
6. IGTP Institut d'Investigació Germans Trias I Pujol, Badalona, Barcelona, Spain
7. CIBERINFEC, ISCIII - CIBER de Enfermedades Infecciosas, Instituto de Salud Carlos III, Majadahonda, Madrid, Spain

### **Correspondence:**

Ana-Paula Dantas. Experimental Cardiology. Institut d'Investigacions Biomèdiques August Pi i Sunyer (IDIBAPS). C/ Casanova 143. Cellex, Planta 2 Sector A. 08036, Barcelona, Spain.

Tel: +34 932274500 Ext 4899. [apvilleladantas@ub.edu](mailto:apvilleladantas@ub.edu)

## **Expanded Materials & Methods**

### **Sample collection and Extracellular Vesicles (EVs) isolation**

Blood samples were collected in a 10-mL EDTA tube during PCI (after reperfusion) in NSTEMI patients and by venipuncture in control volunteers. Samples were immediately sent (within 1h) to the laboratory for plasma obtention. Plasma samples were prepared using the centrifugation protocol recommended by the International Society on Thrombosis and Haemostasis (ISTH). First centrifugation was done at 2,000g for 15 min, and two-thirds of the supernatant (plasma) was transferred to a new tube and followed a second centrifugation at 2,500g for 15 min to remove any remaining cell debris and platelets. EVs were purified from 1mL aliquot of plasma by a combination of polymer-based precipitation (PBP) and size exclusion chromatography (SEC) . For precipitation, EVs were initially isolated according to the manufacturer-recommended protocols for miRCURY Exosome Serum/Plasma Kit (Qiagen, Hilden Germany). Briefly, samples were thawed on ice, and the corresponding volume of EV precipitation buffer was added proportional to the starting serum volume (1 ml). EV precipitation was performed O.N. at 4°C. EVs pellets were obtained by two sequential centrifugations of 1,500 g for 30 min R.T. and resuspended in 1 ml of sterile Phosphate Buffer Saline (PBS). Following resuspension, particles were separated by size-exclusion chromatography (SEC) with Sepharose CL-2B columns (Sigma–Aldrich, St. Louis, MO, USA) as previously described [9]. Briefly, 1 mL of plasma was applied to a 10 mL column equilibrated with PBS–citrate 0.32% (w/v). Collections of 20 fractions of 0.5 mL each started immediately with PBS–citrate as an elution buffer. Aliquots of fractions F6 to F10 were analysed to identify EV-enriched fractions, and fractions F7 to F9 were subsequently pooled for use in functional studies. Protein concentrations of pulled chromatographic fractions F7-F9 eluates were measured by Bradford assay using a standard curve of bovine serum albumin (BSA) serial dilution.

### **EV characterization and quantitation**

Fractions F6-F10 from the SEC were analyzed by flow cytometry for the presence of antigens CD9, CD63, or CD81, based on a previously published protocol [9]. Isolated F6 to F10 EVs were coupled to 4 µm latex beads (aldehyde-sulphate) in PBS–0.1% BSA 0.01% NaN<sub>3</sub> buffer and incubated overnight at R.T. with primary antibodies for 30 minutes at 4°C. The primary antibodies were used at the following dilutions: 1:500 anti-CD9 (9PU-01MG; Immunostep S.L, Salamanca, Spain), 1:500 anti-CD63 (63PU-01MG; Immunostep S.L, Salamanca, Spain), or 1:500 anti-CD81 (sc-23962; Santa Cruz Biotechnology, Dallas, TX, USA). An isotype anti-IgG was used as the control. Unbound primary antibodies were washed off by centrifugation at 2,000g for 10 min, and the secondary antibody conjugated to FITC at

a 1:100 dilution (1032-02; SouthernBiotech, Birmingham, AL, USA) was incubated with samples for 30 minutes at 4°C. After two washing steps, beads were resuspended in 100 µL of PBS–BSA 0.1%. Samples were analyzed by flow cytometry using a Flux FACSLyric flow cytometer (BD Biosciences, San Jose, CA, USA), 10,000 single beads per sample were examined, and median fluorescence intensity (MFI) was used to compare different fractions. EVs fractions were also characterized by a semi-quantitative antibody array with eight antibodies for known EVs markers (Exo-Check™, System Biosciences, Palo Alto, CA, USA). Particle size and distribution were characterized by nanoparticle tracking analysis using a NanoSight NS300 system (Malvern Instruments, Worcestershire, UK), and EVs concentration in each sample was determined with FluoroCet Exosome Quantitation kit (System Biosciences, Palo Alto, CA, USA), following the manufacturer's protocol.

### **Endothelial cell culture and EVs treatment**

Primary human umbilical vein endothelial (HUVEC) cell line (Thermo Fisher Scientific, Waltham, MA, USA) was maintained in culture in EGM-2 media (Lonza, Basel, Switzerland) supplemented with 10% (v/v) fetal bovine serum (FBS) and growth supplement (Lonza, Basel, Switzerland), and incubated at 37 °C in a humidified atmosphere at 95% air and 5% CO<sub>2</sub>. Cells were plated onto 1% gelatin-coated 6-well culture dishes, and at 70% confluence media was changed to DMEM-F12 supplemented with 5% EV-depleted FBS (Thermo Fisher Scientific, Waltham, MA, USA). After O.N. incubation in EV-free media [EGM-2 media supplemented with 5% (v/v) EV-depleted FBS], cells were individually treated with  $5 \times 10^7$  particles / cm<sup>2</sup> from fractions F7-F9 of each sample of NSTEMI patient or control volunteer. A group of cells treated with purified EVs from HUVEC culture media (n = 8) was considered as Sham treatment group, and a set of untreated cells (NT, n = 8) was used as assay controls.

### **Role of EV treatment on angiogenesis and morphogenesis**

Following 48 hours of incubation with EVs, changes in HUVEC phenotype were determined based on their ability to migrate and undergo angiogenesis.

The migration rate of HUVEC was determined by standardized scratch assay [10]. In this set of experiments, HUVEC were grown in 12-well plate and treated with EVs as described above. Monolayers were manually scraped with a 100µl pipette tip, gently washed twice with PBS to remove non-adherent cells and incubated in media supplemented with 1% EV-depleted FBS to reduce proliferation. Images of the scratched area were taken immediately after (T<sub>0</sub>) and at 6, 12, 24, 36, 48 hours after injury using the x5 objective of an inverted microscope (Axiovert 200 Zeiss, Oberkochen, Germany) and ZEN software. The scratched area was measured using NIH Image J software with MRI Wound Healing Tool, and the percentage of the invaded area was determined as [% Healing =

$100 \cdot (\text{Area T0} - \text{Area TX}) / \text{Area T0}$ ; where Area T0 = initial area (T=0) and Area TX= area at each time (X) h after injury.

The ability of EV-treated ECs to form capillary-like structures was determined by seeding them onto  $\mu$ -Angiogenesis Slides (Ibidi, Martinsried, Germany) coated with factor-reduced Matrigel™ (Corning, New York, NY, USA) [11]. Cells were grown in EGM-2 Media (Lonza, Basel, Switzerland) supplemented with growth bullet kit and 5% EV-depleted FBS for 6 hours in an incubator at 37 °C with 5% CO<sub>2</sub>. Network formation was observed and photographed using an x5 objective in a phase-contrast inverted light microscope (Axiovert 200, Zeiss). Tube formation in the microphotographs was quantitatively analyzed by measuring the number of junctions, segments, and meshes (closed loop) using NIH ImageJ software with the angiogenesis analyzer plugin.

The potential of EVs in vascular morphogenesis was determined by the ability of ECs to disperse throughout a matrix and associate into microvessel-like structures (long branches and anastomoses with lumens of capillary diameter) and to interconnect to form a network. For that purpose, the behavior of HUVEC treated with EVs was tested in a 3D angiogenesis system, according to the protocol described by Nakatsu et al [12]. The day before the assay set up, HUVEC were detached by trypsinization and incubated with collagen-coated Cytodex 3 microcarrier beads (GE Healthcare, Buckinghamshire, UK) at a concentration of 400 cells/bead. Unattached cells were removed by incubation O.N. of cell/bead suspension in a 1 cm<sup>2</sup> tissue culture plate. Bead/cell suspension was recollected in a 15 mL conical tube, washed twice with fresh media by gravity sedimentation, and resuspended in 1mL of fresh EV-free EGM-2 media. Coated beads were manually counted by pipetting and an aliquot (20 $\mu$ l) of bead suspension onto a coverslip, and resuspended in fibrinogen solution (2 mg/ml in PBS) to a concentration of 500 beads/ml. Fibrin matrix was formed by mixing 500 $\mu$ l of fibrinogen/bead solution with 1.25U/ml of fibrin into each well of 24-well plates. Fibrinogen/bead solution was allowed to clot for 5 min at R.T. and then incubated for 30 min at cell culture incubator. Human cardiac fibroblasts (Cell Applications, Inc, San Diego, CA, USA) were seed at a concentration of 20,000 cells/ml of EV-free EGM-2 media on top of the fibrin/bead gel to provide factors that synergize with ECs to promote optimal vascular morphogenesis. The cocultures were incubated for seven days, changing the medium every other day. Branches formation throughout the fibrin scaffold was observed and photographed using an X5 and X10 objectives of a phase-contrast inverted light microscope (Axiovert 200, Zeiss) at days 1, 3, and 7. The number of sprout tips per bead and the length of branches were quantitatively analyzed by NIH ImageJ software.

### **Angiogenesis antibody arrays**

The relative levels of human angiogenesis-related proteins in purified EVs from Control and NSTEMI patients were measured using the Human Angiogenesis Array Kit (R&D Systems Inc, Minneapolis, MN, USA). EVs (100 µg protein) from 4 pulled samples of Control volunteers and 4 pulled samples of NSTEMI patients were incubated with the array according to the manufacturer's instructions. Following recommended incubations and washes, the chemiluminescent signal in each membrane was visualized by the LAS4000 imaging system (GE Healthcare, Buckinghamshire, UK). Densitometric analyses of phosphorylation signals were performed using ImageJ software and normalized by the signal of reference spot in each membrane.

### **Total RNA Isolation and Quantification of miRNA and mRNA**

Total RNA (tRNA) was isolated from 100µl of EV solution fractions using the miRCURY RNA Isolation Kit for Biofluids (Qiagen, Hilden Germany) and from EV-treated ECs with RNeasy Mini Kit (Qiagen, Hilden Germany) following the manufacturer's instructions. Aliquots were assessed for quality and quantity with a chip for Small RNA with the Agilent 2100 Bioanalyzer (Agilent Technologies, Santa Clara, CA) and by Invitrogen™ Qubit™ 3.0 Fluorometer (Thermo Fisher, Waltham, MA) respectively. For miRNA analysis, equal amounts of miRNA (10ng) were used for reverse transcription and preamplification using the TaqMan™ Advanced miRNA Reverse Transcription Kit (Applied Biosystems, Thermo Fisher, Waltham, MA). The expression of 754 unique miRNA was determined in randomly pooled EVs samples from control (n=4) and NSTEMI (n=10) by TaqMan™ OpenArray™ Human Advanced MicroRNA Panel (Applied Biosystems, Thermo Fisher, Waltham, MA). mRNA expression of 178 genes involved in angiogenesis and vascular morphogenesis was determined in randomly pooled samples of tRNA isolated from Sham-treated HUVEC (n=4) and cells treated with EVs from control (n=4) and NSTEMI (n=4). One µg of pooled RNA was reversed transcribed into cDNA with High-Capacity cDNA Reverse Transcription Kit (Applied Biosystems, Thermo Fisher, Waltham, MA) and mRNA expression was determined with TaqMan™ Human Immune and Angiogenesis Panels (Applied Biosystems, Thermo Fisher, Waltham, MA). The expression of both miRNA and mRNA was calculated according to the  $\Delta\Delta C_t$  method considering a pull of RNA from control samples (EV) or sham (cells) as a reference. Relative quantification was performed using QuantStudio™ Software and expressed as Log<sub>2</sub> of fold change.

### **Interaction of miRNA/mRNA**

Prediction of target genes interaction with miRNA modified in EVs of NSTEMI patients was made with miRNet (<https://www.mirnet.ca/>), an integrated platform linking miRNAs, targets, and functions from 11 databases [13]. The miRNA-mRNA interactions were directly downloaded from the webpage

and plotted for network visualization on Cytoscape Software V3.8. Gene Ontology and Kyoto Encyclopedia of Genes and Genomes pathway analyses were performed using GeneMANIA Database for Visualization and Integration of genes with their molecular function.

### **miRNA Validation in the Entire Study Population**

Expression of the miRNAs miR-125a-5p and miR-199a-3p was determined in the entire cohort by qRT-PCR analysis using the QuantStudio™ PCR System (Applied Biosystem-Thermo Fisher, Waltham, MA, USA). cDNA samples were used for amplification by qRT-PCR using TaqMan™ microRNA Assays (Applied Biosystem-Thermo Fisher, Waltham, MA, USA) of the selected miRNAs and TaqMan 2X Universal PCR Master Mix, No AmpErase UNG (Applied Biosystem-Thermo Fisher, Waltham, MA, USA). Those two miRNAs were chosen for validation in the entire cohort based on significant correlation with changes in mRNA expression in EV-treated HUVECs and associated with the antiangiogenic effect observed in NSTEMI group. miR-16-5p expression was used for normalization purposes, as recommended in miRNA arrays. Each sample was analyzed in duplicate, and expression was calculated according to the  $2^{-\Delta\Delta Ct}$  method considering the average cycle threshold (Ct) value of all control samples as a reference.

### **miRNA-based Therapy**

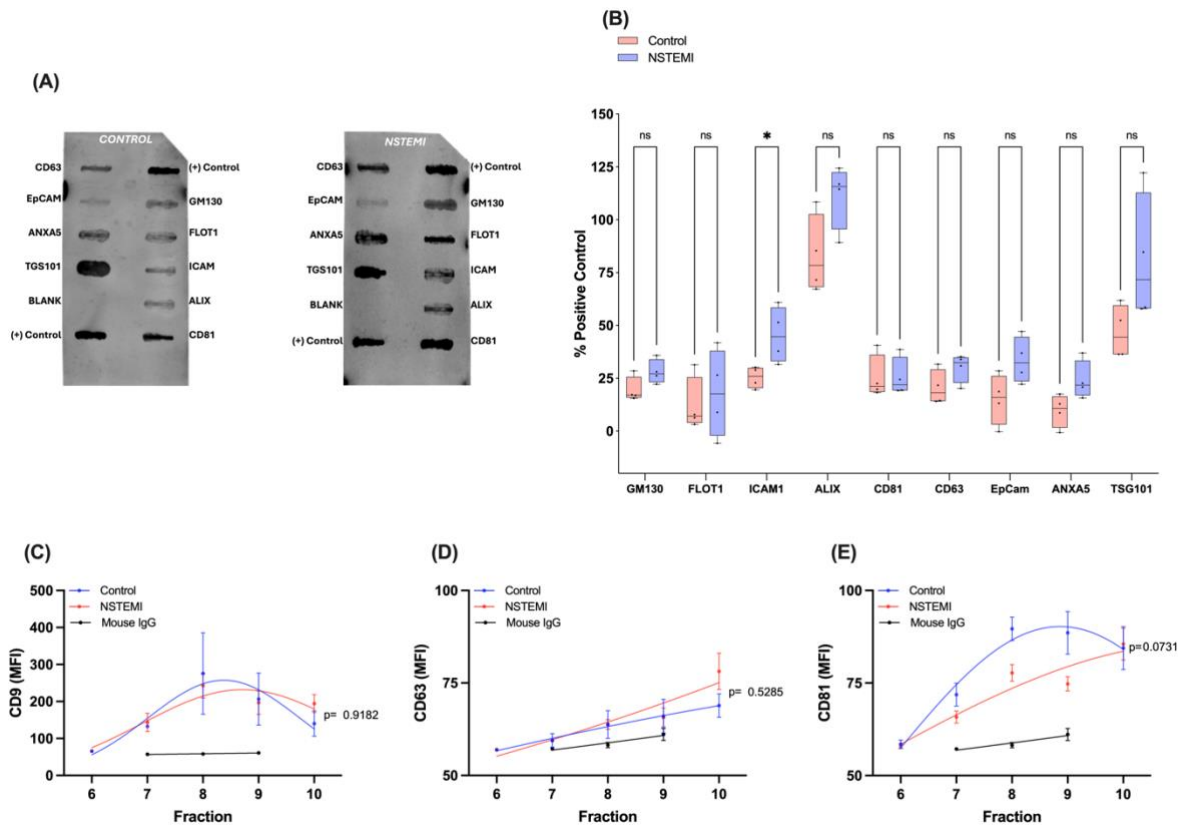
ECs were transfected with miRCURY LNA miRNA mimics and inhibitors for miR-125a-5p and miR-199a-3p labeled at the 5' end with 6-FAM (Qiagen, Hilden Germany). A scrambled oligonucleotide sequence was used as and mimic negative control. ECs were grown in twelve-well plates as described above until reached 70-80% confluency. For transfection, media was changed for Opti-MEM reduced serum media (Gibco, Thermo Fisher Scientific, Waltham, MA, USA) with 1% FBS and without antibiotics or growth supplements. A final concentration of 20nM of miRNA oligonucleotides (mimic, inhibitors, and scramble) were transfected into ECs with DharmaFECT Duo Transfection Reagent (Dharmacon, Colorado, USA) according to the manufacturer instructions. Transfection efficiency was evaluated by visualization of cell fluorescence using the Axiovert 200 fluorescent microscope with Axio Cam MRm and ZEN software (Zeiss, Oberkochen, Germany). The optimal conditions for transfection were determined in preliminary studies to establish the concentration that produces a transfection efficiency greater than 80% without causing toxicity. After incubation O.N., transfection media was replaced by complete endothelial cell media (described above) and cells were incubated for additional 24 h before performing 3D angiogenesis assay. The effects of miRNAs on EC phenotype were studied by treating cells with miRNA alone (miR-125a-5 or miR-199a-3p) or in combination (miR-125a-5 + miR-199a-3p). To determine the effects of miRNA inhibition on the actions of NSTEMI EVs, ECs were treated

with anti-miRNA (anti-miR-125a-5p, anti-miR-199a-3p or a combination of both inhibitors), along with treatments of a pull of EVs from NSTEMI patients, randomly mixed into different groups.

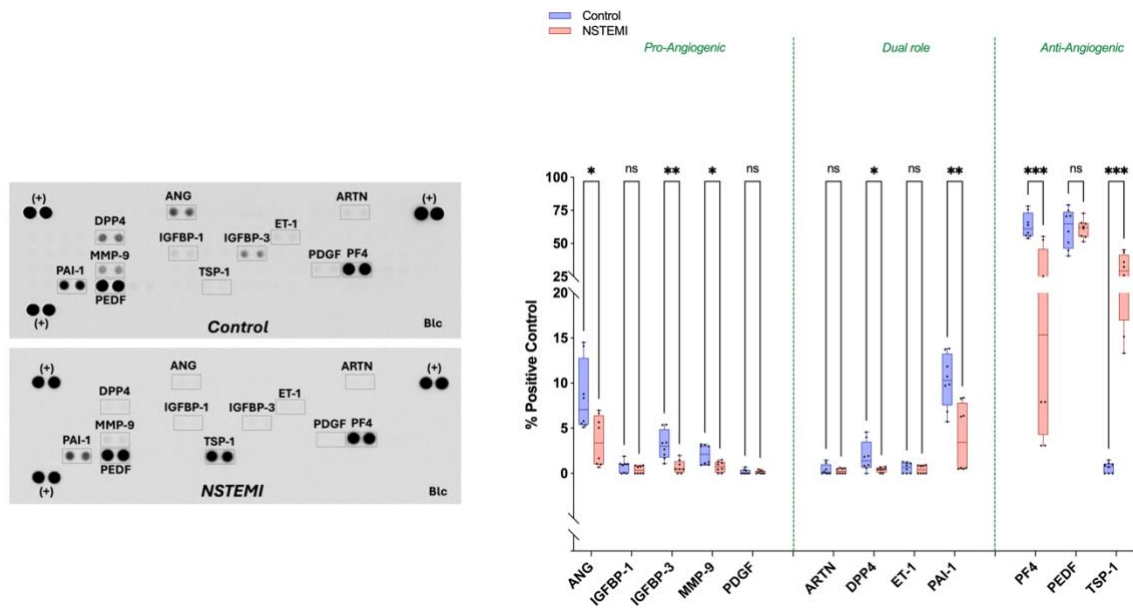
## References

9. de Menezes-Neto, A., et al., *Size-exclusion chromatography as a stand-alone methodology identifies novel markers in mass spectrometry analyses of plasma-derived vesicles from healthy individuals*. J Extracell Vesicles, 2015. **4**: p. 27378.
10. Ciudad, P., et al., *K<sup>+</sup> channels expression in hypertension after arterial injury, and effect of selective Kv1.3 blockade with PAP-1 on intimal hyperplasia formation*. Cardiovasc Drugs Ther, 2014. **28**(6): p. 501-11.
11. Mompeon, A., et al., *Circulating miRNA Fingerprint and Endothelial Function in Myocardial Infarction: Comparison at Acute Event and One-Year Follow-Up*. Cells, 2022. **11**(11).
12. Nakatsu, M.N. and C.C. Hughes, *An optimized three-dimensional in vitro model for the analysis of angiogenesis*. Methods Enzymol, 2008. **443**: p. 65-82.
13. Fan, Y., et al., *miRNet - dissecting miRNA-target interactions and functional associations through network-based visual analysis*. Nucleic Acids Res, 2016. **44**(W1): p. W135-41.

## Supplementary Figures

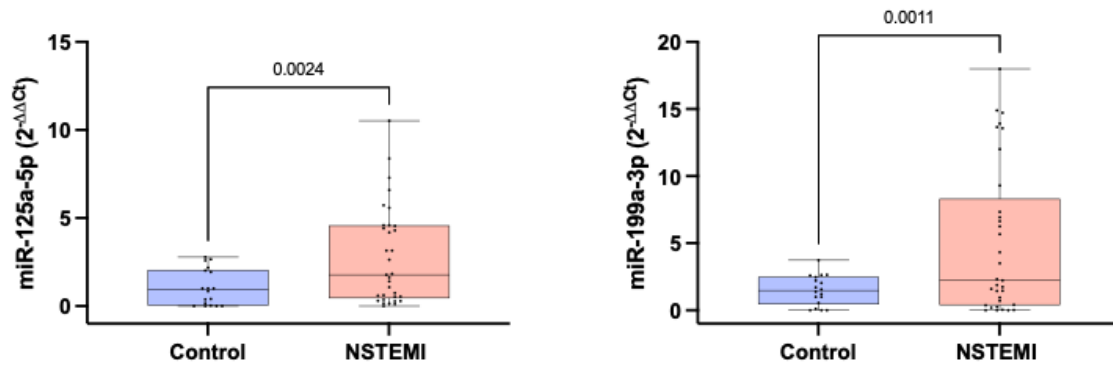


**Supplementary Figure I. Molecular characterization of plasma-derived EVs.** Representative image of EVs' markers array membranes used to characterize EVs profile of samples from healthy control and NSTEMI patients **(A)**. Box and whisker plots shows the mean and the distribution of relative expression of EVs markers in Control and NSTEMI groups **(B)**. Fractions 6-10 of EVs purified by size exclusion chromatography (SEC) were analyzed by flow cytometry bead-based assay. X-Y plots show the mean fluorescence intensity (MFI) of CD9 **(C)**, CD63 **(D)** and CD81 **(E)** markers in SEC fractions from particles precipitated from plasma of Control volunteers and NSTEMI Negative Control (Mouse IgG) refers to a mix of all fractions incubated with anti-mouse Alexa 488- secondary antibody. Differences in the expression of EVs markers in the array between Control and NSTEMI groups were analyzed by multiple T-test with false discovery rate (FDR) correction using the method of Benjamini and Hochberg. Repeated measure 2-way ANOVA analyzed the dependence of data of each EV marker in each SEC fraction with the two different experimental groups (Control vs NSTEMI). \*  $p < 0.05$ , \*\*  $p < 0.01$ , \*\*\*  $p < 0.001$ , ns – nonsignificant. Significance is considered when  $p < 0.05$ .



**Supplementary Figure II. Extracellular vesicles content of angiogenesis-associated proteins.**

Representative image of angiogenesis antibody array membranes used to measure the angiogenic profile of EVs from NSTEMI patients and healthy control **(A)**. Violin plot shows the distribution - with median (long dash) and quartiles (dotted line) - of relative expression of angiogenesis-associated markers of EVs from Control and NSTEMI groups **(B)**. T-test with Welch's determined significant differences among means. \*  $p < 0.05$ , \*\*  $p < 0.01$ , \*\*\*  $p < 0.001$ , ns – nonsignificant. Significance is considered when  $p < 0.05$ . Significance was considered when  $p < 0.05$ .



**Supplementary Figure III. Validation of EVs-derived miR-125a-5p and miR-199a-3p expression in the study population.** Comparison of miRNA expression in EVs isolated from control subjects (n =19) and NSTEMI patients (n = 33). Box and whisker plot shows the mean and distribution of the fold change ( $2^{-\Delta\Delta Ct}$ ) of the selected miRNAs, considering the average delta Ct of miRNA from control samples as a reference. P values of unpaired T-test with Welch's are expressed on top of each violin plot group set. Significance was considered when  $p < 0.05$ .

**Supplementary Table 1 - Statistics and differential gene expression in TaqMan™ Human Immune and Angiogenesis Panels.**  
**Listed are genes that were detected in NSTEMI group relative to the values obtained in Control group.**

Assay ID	Gene Symbol	Alternative Symbol	Name	FC (Log2) Control	SE Difference Control	p Value (Control)	FDR (Control)	FC (Log2) NSTEMI	SE Difference NSTEMI	p Value (NSTEMI)	FDR (NSTEMI)	SE Difference NSTEMI vs Control	p Value (NSTEMI)	FDR (NSTEMI)
Hs99999901_s1	18S		18S ribosomal RNA	0	0			0	0			0		
Hs00174179_m1	ACE		ANGIOTENSIN I-CONVERTING ENZYME	0.821	1.659	0.628425	0.593664	-0.2678	1.562	0.866338	0.8842	-1.089	0.31754	0.304954
Hs99999903_m1	ACTB		ACTIN, BETA	0	0			0	0			0		
Hs00199608_m1	ADAMTS1		A DISINTEGRIN-LIKE AND METALLOPROTEINASE WITH THROMBOSPONDIN TYPE 1 MOTIF, 1	2.602	0.7241	0.002936	0.030652	-3.736	1.685	0.043633	0.0822	-6.338	0.001929	0.013176
Hs00241341_m1	AGTR1		ANGIOTENSIN RECEPTOR 1	0	0			0	0			0		
Hs00169126_m1	AGTR2		ANGIOTENSIN II RECEPTOR, TYPE 2	0	0			0	0			0		
Hs00611096_m1	AMOT		ANGIOMOTIN	-0.1055	1.566	0.947232	0.710424	-6.167	0.6177	0.000001	1E-06	-6.061	0.001096	0.012305
Hs02379000_s1	ANG		ANGIOGENIN; RIBONUCLEASE A FAMILY 5	3.175	1.513	0.054524	0.109047	-5.135	2.83	0.09107	0.1441	-8.31	0.011924	0.025379
Hs00181613_m1	ANGPT1	ANG1	ANGIOPOIETIN 1	0.5923	1.69	0.731261	0.639853	-2.712	0.9074	0.009761	0.0458	-3.305	0.044562	0.068808
Hs00169867_m1	ANGPT2	ANG2	ANGIOPOIETIN 2	-4.382	1.336	0.005479	0.032125	-2.997	1.561	0.075438	0.1272	1.385	0.481357	0.400343
Hs00907078_m1	ANGPT4		ANGIOPOIETIN 4	0	0			0	0			0		
Hs00559786_m1	ANGPTL1		ANGIOPOIETIN-LIKE 1	0	0			0	0			0		
Hs00765775_m1	ANGPTL2		ANGIOPOIETIN-LIKE 2	0.398	1.642	0.811949	0.656673	-3.243	1.002	0.005958	0.0415	-3.641	0.023075	0.045429
Hs00205581_m1	ANGPTL3		ANGIOPOIETIN-LIKE 3	0	0			0	0			0		
Hs01101127_m1	ANGPTL4		ANGIOPOIETIN-LIKE 4	-0.6685	1.598	0.681966	0.61597	-3.35	1.629	0.058913	0.1038	-2.682	0.254741	0.257624
Hs01105174_m1	BAI1		ADHESION G PROTEIN-COUPLED RECEPTOR B1	0	0			0	0			0		
Hs00180269_m1	BAX		BCL2-ASSOCIATED X PROTEIN	1.821	0.6028	0.009163	0.032125	-5.016	1.991	0.024545	0.0458	-6.837	0.003179	0.013176
Hs00153350_m1	BCL2		B-CELL CLL/LYMPHOMA 2	1.279	1.834	0.496964	0.509085	2.343	1.859	0.228253	0.3077	1.064	0.342925	0.325366
Hs00169141_m1	BCL2L1	BCLX	BCL2-LIKE 1	0.8488	1.793	0.643175	0.5937	-4.311	0.9259	0.000371	0.0045	-5.16	0.005218	0.015806
Hs00163811_m1	C3		COMPLEMENT COMPONENT 3	0	0			0	0			0		
Hs00171149_m1	CCL19		CHEMOKINE, CC MOTIF, LIGAND 19	3.118	1.981	0.137839	0.214416	-1.768	2.764	0.532772	0.606	-4.886	0.057314	0.083741
Hs00234140_m1	CCL2	MCP1	CHEMOKINE, CC MOTIF, LIGAND 2	-6.491	1.703	0.001907	0.026477	-3.362	1.238	0.016781	0.0458	3.13	0.157118	0.180228
Hs00234142_m1	CCL3		CHEMOKINE, CC MOTIF, LIGAND 3	0	0			0	0			0		
Hs00174575_m1	CCL5		CHEMOKINE, CC MOTIF, LIGAND 5	-0.5583	1.315	0.677693	0.61597	-0.7548	1.681	0.660262	0.721	-0.1965	0.89592	0.665601
Hs00174150_m1	CCR2		CHEMOKINE, CC MOTIF, RECEPTOR 2	0	0			0	0			0		
Hs99999919_m1	CCR4		CCR4-NOT TRANSCRIPTION COMPLEX, SUBUNIT 6	9.451	3.155	0.009629	0.032125	-1.42	4.466	0.755183	0.7854	-10.87	0.00705	0.017832
Hs00152917_m1	CCR5		CHEMOKINE, CC MOTIF, RECEPTOR 5	0	0			0	0			0		
Hs00171054_m1	CCR7		CHEMOKINE, CC MOTIF, RECEPTOR 7	0	0			0	0			0		
Hs00174333_m1	CD19		B-LYMPHOCYTE ANTIGEN	0	0			0	0			0		
Hs00174796_m1	CD28		T-CELL ANTIGEN	0	0			0	0			0		
Hs00156373_m1	CD34		HEMATOPOIETIC PROGENITOR CELL ANTIGEN	-0.3105	1.254	0.808018	0.656673	-1.599	2.227	0.48466	0.563	-1.288	0.552026	0.448165
Hs00233552_m1	CD38		ADP-RIBOSYL CYCLASE/CYCLIC ADP-RIBOSE HYDROLASE ECTO-NICOTINAMIDE ADENINE DINUCLEOTIDE GLYCOHYDROLASE	0	0			0	0			0		
Hs00167894_m1	CD3E		T-CELL ANTIGEN RECEPTOR COMPLEX, EPSILON SUBUNIT OF T3	0	0			0	0			0		
Hs00181217_m1	CD4		T-CELL ANTIGEN T4	0	0			0	0			0		
Hs00374176_m1	CD40		B CELL-ASSOCIATED MOLECULE CD40; TUMOR NECROSIS FACTOR RECEPTOR SUPERFAMILY	0.713	2.003	0.727118	0.639853	-0.1883	1.695	0.91312	0.8991	-0.9013	0.482954	0.400343
Hs00163934_m1	CD40LG		CD40 ANTIGEN LIGAND	0	0			0	0			0		
Hs00153304_m1	CD44		CD44 ANTIGEN	1.134	0.5765	0.069426	0.135624	-5.167	1.728	0.009729	0.0458	-6.301	0.002034	0.013176
Hs00154355_m1	CD68		MACROPHAGE ANTIGEN CD68	-0.6338	2.208	0.778278	0.656673	-3.328	1.354	0.027646	0.0481	-2.694	0.157914	0.180228
Hs00175478_m1	CD80		CD28 ANTIGEN LIGAND 1	0	0			0	0			0		
Hs00199349_m1	CD86		CD28 ANTIGEN LIGAND 2	0	0			0	0			0		
Hs00233520_m1	CD8A		OKT8 T-CELL ANTIGEN	0	0			0	0			0		
Hs00174344_m1	CDH5	VE-CADHERI	CADHERIN 5	1.431	0.4969	0.012142	0.033767	-6.052	2.08	0.011413	0.0458	-7.482	0.002398	0.013176
Hs00236077_m1	CEACAM1		CARCINOEMBRYONIC ANTIGEN-RELATED CELL ADHESION MOLECULE 1	1.662	1.544	0.300061	0.355002	-2.912	2.297	0.225563	0.3077	-4.573	0.04454	0.068808
Hs00900373_m1	CHGA		CHROMOGRANIN A	0	0			0	0			0		
Hs01559630_m1	COL15A1		COLLAGEN, TYPE XV, ALPHA-1	0	0			0	0			0		
Hs01043425_g1	COL18A1		COLLAGEN, TYPE XVIII, ALPHA-1	-2.428	1.851	0.210756	0.282017	-1.46	1.526	0.355008	0.4456	0.968	0.536762	0.440313
Hs01007469_m1	COL4A1		COLLAGEN, TYPE IV, ALPHA-1	1.549	0.3814	0.001165	0.024459	-4.934	2.045	0.03013	0.0621	-6.484	0.006555	0.017207
Hs01098873_m1	COL4A2		COLLAGEN, TYPE IV, ALPHA-2	0.07325	0.6953	0.917587	0.694711	-4.652	1.776	0.020216	0.0458	-4.726	0.025429	0.047679
Hs01022527_m1	COL4A3		COLLAGEN, TYPE IV, ALPHA-3	0	0			0	0			0		
Hs00166712_m1	COL4A5		COLLAGEN, TYPE IV, ALPHA-5	-1.109	1.995	0.587083	0.580176	-4.598	1.545	0.010007	0.0458	-3.489	0.132342	0.160338
Hs00174164_m1	CSF1		COLONY-STIMULATING FACTOR 1	-2.013	1.726	0.262897	0.334319	-3.147	1.089	0.011913	0.0458	-1.134	0.437155	0.38251
Hs00171266_m1	CSF2		COLONY-STIMULATING FACTOR 2	0	0			0	0			0		
Hs999999083_m1	CSF3		COLONY-STIMULATING FACTOR 3	-0.4475	1.56	0.778374	0.656673	-2.639	1.403	0.081069	0.1321	-2.191	0.029743	0.051191
Hs00170014_m1	CTGF		CONNECTIVE TISSUE GROWTH FACTOR	1.588	0.5577	0.012905	0.033767	-6.23	2.439	0.022953	0.0458	-7.818	0.005688	0.016591
Hs00175480_m1	CTLA4		CYTOTOXIC LYMPHOCYTE-ASSOCIATED 4	0	0			0	0			0		
Hs00171042_m1	CXCL10		CHEMOKINE, CXC MOTIF, LIGAND 10	0.5675	2.354	0.813023	0.656673	-5.053	3.263	0.143762	0.2151	-5.62	0.073213	0.102955
Hs00171138_m1	CXCL11		CHEMOKINE, CXC MOTIF, LIGAND 11	0.6435	2.055	0.758835	0.656673	0.236	1.71	0.892225	0.8991	-0.4075	0.743155	0.573759
Hs00171022_m1	CXCL12	SDF1	CHEMOKINE, CXC MOTIF, LIGAND 12	1.078	1.423	0.461574	0.478669	-2.34	2.372	0.340628	0.4325	-3.417	0.093443	0.126873
Hs00601975_m1	CXCL2		CHEMOKINE, CXC MOTIF, LIGAND 2	-2.138	1.908	0.281416	0.341465	-6.543	0.792	0.000001	1E-06	-4.405	0.026648	0.048803
Hs00171041_m1	CXCR3		CHEMOKINE, CXC MOTIF, RECEPTOR 3	0	0			0	0			0		
Hs00167927_m1	CYP1A2		CYTOCHROME P450, SUBFAMILY I, POLYPEPTIDE 2	4.011	1.287	0.007584	0.032125	-0.5423	3.027	0.860387	0.8842	-4.553	0.142557	0.167557
Hs00167982_m1	CYP7A1		CYTOCHROME P450, SUBFAMILY VIIA, POLYPEPTIDE 1	0	0			0	0			0		
Hs00154837_m1	ECE1		ENDOTHELIN-CONVERTING ENZYME 1	1.1	0.4281	0.022267	0.053441	-5.11	1.877	0.0165	0.0458	-6.21	0.004459	0.015253
Hs00157317_m1	ECGF1		ENDOTHELIAL CELL GROWTH FACTOR, PLATELET-DERIVED	2.514	1.397	0.093504	0.169087	-0.224	2.278	0.923069	0.9	-2.738	0.216475	0.233526
Hs01922614_s1	EDG1	S1PR1	SPHINGOSINE-1-PHOSPHATE RECEPTOR 1	4.636	1.503	0.008083	0.032125	1.526	2.006	0.459679	0.5398	-3.111	0.040236	0.066013
Hs00174781_m1	EDIL3		EGF-LIKE REPEATS- AND DISCOIDIN I-LIKE DOMAINS-CONTAINING PROTEIN 3	1.365	0.4817	0.013265	0.033767	-4.092	1.58	0.021415	0.0458	-5.457	0.004357	0.015253
Hs00174961_m1	EDN1		ENDOTHELIN 1	0.5903	0.4315	0.192894	0.270904	-5.09	1.993	0.022298	0.0458	-5.68	0.012348	0.025589
Hs00196470_m1	ENPP2		ECTONUCLEOTIDE PYROPHOSPHATASE/PHOSPHODIESTERASE 2	1.741	1.696	0.322225	0.375485	1.796	1.788	0.33239	0.427	0.05475	0.965597	0.678935
Hs00362096_m1	EPHB2		EPHRYN RECEPTOR EphB2	1.652	0.5578	0.010326	0.032125	-4.923	1.875	0.019966	0.0458	-6.574	0.002833	0.013176
Hs01011995_g1	F2		THROMBIN	5.449	1.692	0.006153	0.032125	8.081	5.373	0.154792	0.2267	2.632	0.63607	0.504342
Hs00163653_m1	FAS	CD95; APO1	FAS CELL SURFACE DEATH RECEPTOR	-0.433	2.147	0.843071	0.674457	-3.226	1.267	0.02325	0.0458	-2.793	0.139711	0.166701
Hs00181225_m1	FASLG	CD95L; CD17	FAS LIGAND	4.011	1.287	0.007584	0.032125	5.975	4.158	0.172749	0.2418	1.964	0.638351	0.504342
Hs00197064_m1	FBLN5		FIBULIN 5; DEVELOPMENTAL ARTERIES AND NEURAL CREST EGF-LIKE	1.484	0.7983	0.084274	0.157311	-5.019	1.485	0.004484	0.049	-6.503	0.000408	0.009577
Hs00241027_m1	FGA		FIBRINOGEN, A ALPHA POLYPEPTIDE	0	0			0	0			0		
Hs00265254_m1	FGF1		FIBROBLAST GROWTH FACTOR 1;	-2.654	1.48	0.094608	0.169087	-1.852	1.963	0.36143	0.4485	0.8015	0.725125	0.565382
Hs00266645_m1	FGF2		FIBROBLAST GROWTH FACTOR 2	0.594	1.214	0.632159	0.593664	-2.764	1.462	0.079657	0.1318	-3.358	0.09842	0.131366
Hs00173564_m1	FGF4		FIBROBLAST GROWTH FACTOR 4	0	0			0	0			0		

Hs00189521_m1	FIGF	VEGFD	FOS-INDUCED GROWTH FACTOR; VASCULAR ENDOTHELIAL GROWTH FACTOR D	-1.299	1.611	0.433327	0.456913	-3.282	2.358	0.185658	0.2566	-1.983	0.34973	0.327872
Hs00176573_m1	FLT1	VEGFR1	FMS-RELATED TYROSINE KINASE 1; VASCULAR ENDOTHELIAL GROWTH FACTOR RECEPTOR 1	0.2055	0.7853	0.797379	0.656673	-5.042	1.564	0.006127	0.0415	-5.248	0.004015	0.015253
Hs00174690_m1	FLT3	FLK2	FMS-RELATED TYROSINE KINASE 3; STEM CELL TYROSINE KINASE 1	4.144	1.295	0.006408	0.032125	1.291	2.236	0.572858	0.6383	-2.853	0.202771	0.224904
Hs01047677_m1	FLT4		FMS-LIKE TYROSINE KINASE 4; VASCULAR ENDOTHELIAL GROWTH FACTOR RECEPTOR 3	-1.343	1.601	0.41573	0.453524	-0.6425	1.505	0.675918	0.7236	0.7005	0.480786	0.400343
Hs01549940_m1	FN1	VEGFR3	FIBRONECTIN 1	0.8004	0.4563	0.101305	0.177284	-5.275	1.929	0.016132	0.0458	-6.075	0.006453	0.017207
Hs00270951_s1	FOXC2		FORKHEAD BOX C2	-0.244	1.871	0.898091	0.694711	-3.251	1.629	0.06572	0.1139	-3.007	0.222018	0.235949
Hs00246256_m1	FST		FOLLISTATIN	-1.899	1.478	0.219773	0.288452	-3.223	1.042	0.007963	0.0458	-1.324	0.258666	0.257847
Hs99999905_m1	GAPDH		GLYCERALDEHYDE-3-PHOSPHATE DEHYDROGENASE	0	0			0	0			0		
Hs00246266_m1	GNLV		GRANULYIN	0	0			0	0			0		
Hs00963711_g1	GRN		GRANULIN PRECURSOR	-0.2205	2.104	0.91801	0.694711	-2.593	1.768	0.164622	0.2363	-2.372	0.366266	0.339335
Hs99999908_m1	GUSB		BETA-GLUCURONIDASE	-2.335	1.709	0.193503	0.270904	-4.292	1.487	0.011969	0.0458	-1.957	0.383017	0.344916
Hs00188051_m1	GZMB		GRANZYME B	0	0			0	0			0		
Hs00232618_m1	HEY1		HAIRY/ENHANCER OF SPLIT-RELATED WITH YRPW MOTIF 1	3.136	1.046	0.009585	0.032125	-3.63	1.892	0.075699	0.1272	-6.765	0.001328	0.012305
Hs00300159_m1	HGF		HEPATOCTYE GROWTH FACTOR	0	0			0	0			0		
Hs00219575_m1	HLA-DRA		MAJOR HISTOCOMPATIBILITY COMPLEX, CLASS II, DR ALPHA	0	0			0	0			0		
Hs99999917_m1	HLA-DRB1		MAJOR HISTOCOMPATIBILITY COMPLEX, CLASS II, DR BETA-1	0	0			0	0			0		
Hs00157965_m1	HMOX1		HEME OXYGENASE 1	-1.881	1.413	0.204425	0.281503	-2.002	0.9376	0.0509	0.0911	-0.1215	0.914491	0.666816
Hs01078536_m1	HSPG2		HEPARAN SULFATE PROTEOGLYCAN OF BASEMENT; PERLECAN	-0.2338	0.4724	0.628428	0.593664	-4.61	1.703	0.017003	0.0458	-4.376	0.024598	0.047246
Hs00164932_m1	ICAM1	CD54	INTERCELLULAR ADHESION MOLECULE 1	-2.27	1.372	0.120151	0.197896	-2.522	0.9985	0.024236	0.0458	-0.2518	0.809535	0.612989
Hs00359999_m1	ICOS		INDUCIBLE T-CELL COSTIMULATOR	0	0			0	0			0		
Hs01077958_s1	IFNB1		INTERFERON, BETA-1	4.363	2.995	0.167233	0.250849	-4.371	3.852	0.275574	0.367	-8.734	0.029259	0.051191
Hs00174143_m1	IFNG		INTERFERON, GAMMA	0	0			0	0			0		
Hs00395088_m1	IKKB	IKKB	INHIBITOR OF KAPPA LIGHT CHAIN GENE ENHANCER IN B CELLS	0.5945	0.6556	0.379836	0.425416	-3.832	1.398	0.015903	0.0458	-4.426	0.011528	0.025217
Hs00174086_m1	IL10		INTERLEUKIN 10	7.406	2.52	0.010771	0.032314	7.554	7.259	0.315718	0.4104	0.148	0.984612	0.686178
Hs00168405_m1	IL12A		INTERLEUKIN 12-ALPHA	0.857	1.772	0.636069	0.593664	-4.204	2.286	0.087146	0.1399	-5.061	0.009127	0.021781
Hs00233688_m1	IL12B		INTERLEUKIN 12B	0	0			0	0			0		
Hs00174379_m1	IL13		INTERLEUKIN 13	0	0			0	0			0		
Hs00174106_m1	IL15		INTERLEUKIN 15	2.58	1.602	0.129623	0.205472	1.344	2.088	0.530166	0.606	-1.236	0.445965	0.385368
Hs00174383_m1	IL17		INTERLEUKIN 17	0	0			0	0			0		
Hs00155517_m1	IL18		INTERLEUKIN 18	1.831	1.582	0.266659	0.334319	0.1878	2.428	0.939456	0.9079	-1.643	0.450208	0.385368
Hs00174092_m1	IL1A		INTERLEUKIN 1-ALPHA	-4.398	1.243	0.003284	0.030652	-5.553	0.5157	0.000001	1E-06	-1.154	0.382251	0.344916
Hs00174097_m1	IL1B		INTERLEUKIN 1-BETA	1.684	1.513	0.284554	0.341465	-0.8475	2.484	0.737991	0.7824	-2.532	0.274702	0.27041
Hs00174114_m1	IL2		INTERLEUKIN 2	4.011	1.287	0.007584	0.032125	4.548	5.654	0.434604	0.5159	0.5375	0.924931	0.668241
Hs00166229_m1	IL2RA		INTERLEUKIN 2 RECEPTOR, ALPHA	0	0			0	0			0		
Hs00174117_m1	IL3		INTERLEUKIN 3	0	0			0	0			0		
Hs00174122_m1	IL4		INTERLEUKIN 4	0	0			0	0			0		
Hs00174200_m1	IL5		INTERLEUKIN 5	0	0			0	0			0		
Hs00174131_m1	IL6		INTERLEUKIN 6	1.071	1.878	0.577488	0.577488	-0.9963	1.782	0.58498	0.6453	-2.067	0.311217	0.302572
Hs00174202_m1	IL7		INTERLEUKIN 7	0	0			0	0			0		
Hs00174103_m1	IL8		INTERLEUKIN 8	1.369	0.4474	0.008482	0.032125	-4.052	1.618	0.025218	0.0459	-5.422	0.004565	0.015253
Hs00174125_m1	IL9		INTERLEUKIN 9	0	0			0	0			0		
Hs00168433_m1	ITGA4		INTEGRIN, ALPHA-4	2.223	0.5946	0.002206	0.026477	-4.983	1.828	0.016432	0.0458	-7.205	0.001102	0.012305
Hs00233808_m1	ITGAV		INTEGRIN, ALPHA-V	1.257	0.5644	0.042885	0.092367	-5.144	1.867	0.01547	0.0458	-6.401	0.003088	0.013176
Hs01001469_m1	ITGB3		INTEGRIN, BETA-3	1.898	0.6695	0.013248	0.033767	-4.522	1.926	0.034124	0.0678	-6.42	0.004649	0.015253
Hs00176676_m1	KDR	VEGFR2	KINASE INSERT DOMAIN RECEPTOR; VASCULAR ENDOTHELIAL GROWTH FACTOR RECEPTOR 2	1.559	0.5473	0.012894	0.033767	-3.999	1.516	0.019465	0.0458	-5.558	0.002764	0.013176
Hs00174029_m1	KIT	SCFR	KIT PROTOONCOGENE, RECEPTOR TYROSINE KINASE; STEM CELL FACTOR RECEPTOR	2.15	0.6914	0.007682	0.032125	-3.981	1.367	0.011354	0.0458	-6.131	0.000486	0.009577
Hs00993254_m1	LECT1		LEUKOCYTE CELL-DERIVED CHEMOTAXIN 1	0	0			0	0			0		
Hs00174877_m1	LEP		LEPTIN	0	0			0	0			0		
Hs00189742_m1	LRP2		LOW DENSITY LIPOPROTEIN RECEPTOR-RELATED PROTEIN 2	0	0			0	0			0		
Hs00236874_m1	LTA		LYMPHOTOXIN-ALPHA	0	0			0	0			0		
Hs00171064_m1	MDK		MIDKINE	1.633	0.4982	0.005509	0.032125	-4.155	1.628	0.023031	0.0458	-5.788	0.002542	0.013176
Hs00234422_m1	MMP2		MATRIX METALLOPROTEINASE 2	-0.7083	0.7066	0.333208	0.378236	-4.512	1.777	0.023605	0.0458	-3.804	0.063858	0.091433
Hs00411908_m1	MYH6		MYOSIN, HEAVY CHAIN 6, CARDIAC MUSCLE, ALPHA	0	0			0	0			0		
Hs00174517_m1	NFKB2		NUCLEAR FACTOR KAPPA-B, SUBUNIT 2	-2.153	1.644	0.211513	0.282017	-2.766	1.123	0.027401	0.0481	-0.6133	0.640434	0.504342
Hs00167248_m1	NOS2A	INOS	NITRIC OXIDE SYNTHASE 2A	0	0			0	0			0		
Hs00826128_m1	NRP1		NEUROFILIN 1	-3.162	1.657	0.077008	0.147016	-3.051	1.341	0.039111	0.0763	0.1113	0.959056	0.678935
Hs00187290_m1	NRP2	VEGF165R2	NEUROFILIN 2; VASCULAR ENDOTHELIAL GROWTH FACTOR-165 RECEPTOR 2	-0.3228	0.5025	0.53106	0.537458	-4.793	1.826	0.019989	0.0458	-4.47	0.031523	0.052818
Hs00234042_m1	PDGFB		PLATELET-DERIVED GROWTH FACTOR, BETA POLYPEPTIDE	0.479	0.5835	0.425482	0.456913	-3.896	1.56	0.025606	0.0459	-4.375	0.018314	0.036981
Hs00998026_m1	PDGFRA		PLATELET-DERIVED GROWTH FACTOR RECEPTOR, ALPHA	0	0			0	0			0		
Hs00387364_m1	PDGFRB		PLATELET-DERIVED GROWTH FACTOR RECEPTOR, BETA	0	0			0	0			0		
Hs00169777_m1	PECAM1	CD31	PLATELET-ENDOTHELIAL CELL ADHESION MOLECULE 1	1.784	0.8	0.042609	0.092367	-2.824	1.636	0.106325	0.1659	-4.609	0.009648	0.022036
Hs00427220_g1	PF4		PLATELET FACTOR 4	3.807	1.588	0.031007	0.072351	-1.788	2.975	0.557449	0.6276	-5.595	0.074578	0.103035
Hs99999906_m1	PGK1		PHOSPHOGLYCERATE KINASE 1	-0.00263	0.5142	0.995999	0.740389	-4.629	1.56	0.010198	0.0458	-4.627	0.009794	0.022036
Hs00264877_m1	PLG		PLASMINOGEN	0	0			0	0			0		
Hs00169473_m1	PRF1		PERFORIN 1	0	0			0	0			0		
Hs00168730_m1	PRL		PROLACTIN	0	0			0	0			0		
Hs00260905_m1	PROK1		PROKINETICIN 1	0	0			0	0			0		
Hs00896294_m1	PROX1		PROSPERO-RELATED HOMEBOX 1	2.414	1.14	0.052535	0.107632	-1.936	2.121	0.376859	0.4624	-4.35	0.047617	0.072112
Hs00153133_m1	PTGS2	COX2	PROSTAGLANDIN-ENDOPEROXIDE SYNTHASE 2; CYCLOOXYGENASE 2	-4.541	1.354	0.004733	0.032125	-4.875	0.6953	0.000006	0.0001	-0.3343	0.788611	0.602943
Hs00383235_m1	PTN		PLEIOTROPHIN	3.048	2.168	0.181646	0.267689	-0.811	2.502	0.750651	0.7854	-3.859	0.129558	0.159417
Hs00365634_g1	PTPRC	CD45	PROTEIN-TYROSINE PHOSPHATASE, RECEPTOR-TYPE, C	7.928	2.608	0.008822	0.032125	0.3625	3.292	0.913877	0.8991	-7.566	0.005923	0.016659
Hs00166915_m1	REN		RENIN	0	0			0	0			0		
Hs00192564_m1	RPL3L		RIBOSOMAL PROTEIN L3-LIKE	0	0			0	0			0		
Hs00174057_m1	SELE	E-SELECTIN	SELECTIN E	-0.711	1.423	0.62502	0.593664	-2.428	2.33	0.315065	0.4104	-1.717	0.431115	0.381464
Hs00174583_m1	SELP	P-SELECTIN	SELECTIN P	-2.91	1.807	0.129643	0.205472	-3.118	1.228	0.023608	0.0458	-0.2075	0.880405	0.860304
Hs00188273_m1	SEMA3F		SEMAPHORIN 3F	-3.034	1.779	0.110162	0.186914	-3.19	1.34	0.032051	0.064			

Hs00184728_m1	SERPINB5		PROTEASE INHIBITOR 5	0	0			0	0			0		
Hs00166654_m1	SERPINC1		SERPIN PEPTIDASE INHIBITOR, CLADE C (ANTITHROMBIN), MEMBER 1	-0.499	1.376	0.722348	0.639853	-3.456	2.303	0.155672	0.2267	-2.957	0.191625	0.215578
Hs00171467_m1	SERPINF1		SERPIN PEPTIDASE INHIBITOR, CLADE F, MEMBER 1	2.214	1.5	0.162186	0.247702	-2.701	3.002	0.383463	0.4653	-4.915	0.104165	0.136717
Hs00161707_m1	SKI		SKI PROTOONCOGENE	0.6835	0.4928	0.187174	0.270904	-4.026	1.434	0.013989	0.0458	-4.71	0.00509	0.015806
Hs00232219_m1	SMAD3		SMAD FAMILY MEMBER 3	1.118	0.5055	0.044201	0.092821	-7.108	0.821	0.000001	1E-06	-8.225	<0.000001	0.000002
Hs00178696_m1	SMAD7		SMAD FAMILY MEMBER 7	0.2015	1.765	0.910709	0.694711	-2.903	1.861	0.141103	0.214	-3.104	0.224713	0.235949
Hs00234174_m1	STAT3		SIGNAL TRANSDUCER AND ACTIVATOR OF TRANSCRIPTION 3	1.938	0.86	0.040783	0.092367	-5.871	1.821	0.006117	0.0415	-7.809	0.000433	0.009577
Hs00203436_m1	TBX21		T-BOX TRANSCRIPTION FACTOR 21	0	0			0	0			0		
Hs00176096_m1	TEK	Tie-2	TYROSINE KINASE, ENDOTHELIAL	-0.169	0.9177	0.856527	0.678757	-4.063	0.8728	0.000372	0.0045	-3.894	0.007246	0.017832
Hs99999911_m1	TFRC		TRANSFERRIN RECEPTOR	-1.413	1.677	0.413765	0.453524	-3.376	1.575	0.050189	0.0911	-1.963	0.38543	0.344916
Hs00608187_m1	TGFA		TRANSFORMING GROWTH FACTOR, ALPHA	-2.031	0.7338	0.015101	0.037308	-5.148	2.03	0.023739	0.0458	-3.117	0.12189	0.15482
Hs99999918_m1	TGFB1		TRANSFORMING GROWTH FACTOR, BETA-1	1.058	0.2582	0.001093	0.024459	-2.28	1.383	0.121421	0.1867	-3.337	0.029902	0.051191
Hs00962914_m1	THBS1		THROMBOSPONDIN I	-0.937	0.7884	0.254434	0.328807	-4.246	1.907	0.042949	0.0822	-3.309	0.125088	0.15636
Hs01568063_m1	THBS2		THROMBOSPONDIN II	4.449	1.184	0.002124	0.026477	1.837	2.168	0.411013	0.4932	-2.612	0.21174	0.231591
Hs00178500_m1	TIE1		TYROSINE KINASE WITH IMMUNOGLOBULIN AND EGF FACTOR HOMOLOGY DOMAINS 1	1.748	0.3382	0.000143	0.006003	-4.259	1.539	0.015131	0.0458	-6.007	0.001406	0.012305
Hs00234278_m1	TIMP2		TISSUE INHIBITOR OF METALLOPROTEINASE 2	1.784	0.5238	0.004259	0.032125	-5.017	1.945	0.021849	0.0458	-6.801	0.003114	0.013176
Hs00165949_m1	TIMP3		TISSUE INHIBITOR OF METALLOPROTEINASE 3	1.385	1.724	0.435155	0.456913	-1.081	2.461	0.667137	0.7213	-2.466	0.25517	0.257624
Hs00174128_m1	TNF		TUMOR NECROSIS FACTOR	0	0			0	0			0		
Hs00188346_m1	TNFRSF18		TUMOR NECROSIS FACTOR RECEPTOR SUPERFAMILY, MEMBER 18	0	0			0	0			0		
Hs00270802_s1	TNFSF15		TUMOR NECROSIS FACTOR LIGAND SUPERFAMILY, MEMBER 15	0.4465	1.708	0.797527	0.656673	-2.593	1.777	0.166627	0.2363	-3.04	0.229079	0.237368
Hs00223332_m1	TNMD		TENOMODULIN	0	0			0	0			0		
Hs00913333_m1	TNNI1		TROPONIN I, SLOW-TWITCH SKELETAL MUSCLE ISOFORM	7.978	1.459	0.000083	0.006003	0.4358	3.392	0.899609	0.8991	-7.542	0.043259	0.068808
Hs00208609_m1	VASH1		VASOHIBIN 1	-0.2443	1.474	0.870796	0.683616	-5.732	0.4202	0.000001	1E-06	-5.488	0.002021	0.013176
Hs00900054_m1	VEGF	VEGFA	VASCULAR ENDOTHELIAL GROWTH FACTOR A	-1.574	1.548	0.326314	0.375485	-4.832	0.9163	0.000118	0.0018	-3.257	0.057422	0.083741
Hs00173634_m1	VEGFB		VASCULAR ENDOTHELIAL GROWTH FACTOR B	1.67	0.5625	0.010158	0.032125	-4.348	1.56	0.014561	0.0458	-6.018	0.001391	0.012305
Hs00153458_m1	VEGFC		VASCULAR ENDOTHELIAL GROWTH FACTOR C	-3.028	1.781	0.111258	0.186914	-2.92	1.34	0.046867	0.0867	0.1078	0.936017	0.670103
Hs00272659_m1	XLKD1	LYVE1	LYMPHATIC VESSEL ENDOTHELIAL HYALURONAN RECEPTOR 1	-1.837	1.618	0.275218	0.339975	-3.769	1.326	0.013033	0.0458	-1.931	0.116619	0.150553

**Supplementary Table II - Statistics and differential miRNA expression in TaqMan™ OpenArray™ Human Advanced MicroRNA Panel.**

**Listed are miRNA that were detected in NSTEMI group relative to the values obtained in Control group.**

Array Code	miRBase ID	FC (Log2)	SE of difference	p value	FDR
hsa_let_7a_3p_477861_mir	hsa-let-7a-3p	1.749	3.03	0.571954	0.861366
hsa_let_7a_5p_478575_mir	hsa-let-7a-5p	-1.697	0.9454	0.091664	0.377811
hsa_let_7b_3p_478221_mir	hsa-let-7b-3p	1.242	2.188	0.578177	0.861366
hsa_let_7b_5p_478576_mir	hsa-let-7b-5p	-2.21	0.4998	0.000429	0.026109
hsa_let_7d_3p_477848_mir	hsa-let-7d-3p	-1.57	0.5053	0.006779	0.091743
hsa_let_7d_5p_478439_mir	hsa-let-7d-5p	-3.197	1.634	0.06813	0.319163
hsa_let_7e_5p_478579_mir	hsa-let-7e-5p	-4.317	2.163	0.06331	0.308448
hsa-let-7f-1-3p-477801-mir	hsa-let-7f-1-3p	1.948	2.5	0.447353	0.781777
hsa-let-7f-2-3p-477843-mir	hsa-let-7f-2-3p	0.3035	2.216	0.892752	0.958037
hsa-let-7f-5p-478578-mir	hsa-let-7f-5p	-1.099	2.964	0.715826	0.882403
hsa-let-7g-5p-478580-mir	hsa-let-7g-5p	-0.679	0.4019	0.11053	0.408323
hsa-let-7i-3p-477862-mir	hsa-let-7i-3p	-0.475	1.771	0.79198	0.927531
hsa-let-7i-5p-478375-mir	hsa-let-7i-5p	-0.834	0.4222	0.065763	0.314114
hsa-miR-1-3p-477820-mir	hsa-miR-1-3p	2.795	2.405	0.262124	0.607332
hsa-miR-100-5p-478224-mir	hsa-miR-100-5p	0.341	1.19	0.778041	0.920052
hsa-miR-101-3p-477863-mir	hsa-miR-101-3p	0.4685	0.5148	0.376314	0.73336
hsa-miR-103a-2-5p-477864-mir	hsa-miR-103a-2-5p	4.436	1.666	0.017041	0.143148
hsa-miR-103a-3p-478253-mir	hsa-miR-103a-3p	0.135	2.514	0.957832	0.984506
hsa-miR-106a-5p-478225-mir	hsa-miR-106a-5p	2.704	2.239	0.244752	0.607332
hsa-miR-106b-3p-477866-mir	hsa-miR-106b-3p	-2.433	0.9733	0.023706	0.179603
hsa-miR-106b-5p-478412-mir	hsa-miR-106b-5p	-0.7295	0.4655	0.136608	0.451816
hsa-miR-107-478254-mir	hsa-miR-107	0.1185	0.6203	0.850893	0.955524
hsa-miR-10a-5p-479241-mir	hsa-miR-10a-5p	4.088	1.164	0.002885	0.056276
hsa-miR-10b-5p-478494-mir	hsa-miR-10b-5p	-1.351	0.9231	0.162851	0.48976
hsa-miR-122-5p-477855-mir	hsa-miR-122-5p	-1.026	0.6544	0.136506	0.451816
hsa-miR-1249-3p-478654-mir	hsa-miR-1249-3p	-8.948	2.352	0.001558	0.04218
hsa-miR-125a-5p-477884-mir	hsa-miR-125a-5p	3.72	1.264	0.001436	0.04218
hsa-miR-125b-5p-477885-mir	hsa-miR-125b-5p	1.649	0.8745	0.077723	0.338096
hsa-miR-126-3p-477887-mir	hsa-miR-126-3p	-1.819	0.5624	0.005189	0.074362
hsa-miR-126-5p-477888-mir	hsa-miR-126-5p	-2.396	0.6776	0.002746	0.056276
hsa-miR-1260a-478476-mir	hsa-miR-1260a	-3.848	1.432	0.016196	0.140903
hsa-miR-128-3p-477892-mir	hsa-miR-128-3p	1.638	1.378	0.252155	0.607332
hsa-miR-1282-478683-mir	hsa-miR-1282	-0.0675	2.99	0.982267	0.999646
hsa-miR-129-1-3p-480873-mir	hsa-miR-129-1-3p	0.266	1.481	0.859723	0.95587
hsa-miR-1301-3p-477897-mir	hsa-miR-1301-3p	-2.954	2.495	0.253712	0.607332
hsa-miR-130a-3p-477851-mir	hsa-miR-130a-3p	0.841	1.568	0.599183	0.87385
hsa-miR-130b-3p-477840-mir	hsa-miR-130b-3p	-1.073	1.542	0.496589	0.822918
hsa-miR-130b-5p-477899-mir	hsa-miR-130b-5p	0.3385	1.778	0.851431	0.955524
hsa-miR-133a-3p-478511-mir	hsa-miR-133a-3p	0.896	2.066	0.670251	0.882403
hsa-miR-133b-480871-mir	hsa-miR-133b	0.9345	2.203	0.677121	0.882403
hsa-miR-139-3p-477906-mir	hsa-miR-139-3p	-9.412	3.566	0.017849	0.144931
hsa-miR-139-5p-478312-mir	hsa-miR-139-5p	-3.079	1.98	0.139479	0.453029
hsa-miR-140-3p-477908-mir	hsa-miR-140-3p	3.512	1.966	0.093057	0.377811
hsa-miR-140-5p-477909-mir	hsa-miR-140-5p	-3.172	1.43	0.041366	0.242655
hsa-miR-142-3p-477910-mir	hsa-miR-142-3p	-3.972	0.7379	0.000061	0.007427
hsa-miR-142-5p-477911-mir	hsa-miR-142-5p	-1.542	0.7269	0.049933	0.264427
hsa-miR-143-3p-477912-mir	hsa-miR-143-3p	-1.25	0.7286	0.105545	0.407776
hsa-miR-144-3p-477913-mir	hsa-miR-144-3p	-0.1045	0.5631	0.855107	0.955524
hsa-miR-144-5p-477914-mir	hsa-miR-144-5p	-0.5245	0.4648	0.275781	0.61073

hsa-miR-145-3p-477915-mir	hsa-miR-145-3p	0.244	1.668	0.885497	0.957517
hsa-miR-145-5p-477916-mir	hsa-miR-145-5p	-1.693	0.9071	0.080512	0.344081
hsa-miR-146a-5p-478399-mir	hsa-miR-146a-5p	-1.044	0.483	0.046143	0.249786
hsa-miR-148a-3p-477814-mir	hsa-miR-148a-3p	-0.6995	0.6482	0.296509	0.633593
hsa-miR-148b-3p-477824-mir	hsa-miR-148b-3p	1.274	1.251	0.323958	0.674498
hsa-miR-150-5p-477918-mir	hsa-miR-150-5p	-1.706	0.5139	0.004344	0.066138
hsa-miR-151a-3p-477919-mir	hsa-miR-151a-3p	0.594	1.479	0.693301	0.882403
hsa-miR-151a-5p-478505-mir	hsa-miR-151a-5p	0.8685	1.472	0.563435	0.861366
hsa-miR-151b-477811-mir	hsa-miR-151b	3.281	3.564	0.370894	0.728628
hsa-miR-152-3p-477921-mir	hsa-miR-152-3p	-0.5585	1.515	0.71726	0.882403
hsa-miR-15a-3p-477928-mir	hsa-miR-15a-3p	0.627	1.12	0.583438	0.861366
hsa-miR-15a-5p-477858-mir	hsa-miR-15a-5p	0.318	0.1992	0.129942	0.451816
hsa-miR-15b-3p-477929-mir	hsa-miR-15b-3p	-1.546	0.4425	0.003003	0.056276
hsa-miR-15b-5p-478313-mir	hsa-miR-15b-5p	-0.6775	1.823	0.715101	0.882403
hsa-miR-17-3p-477932-mir	hsa-miR-17-3p	1.341	1.891	0.488665	0.821752
hsa-miR-17-5p-478447-mir	hsa-miR-17-5p	-0.5715	0.3896	0.161808	0.48976
hsa-miR-181a-3p-479405-mir	hsa-miR-181a-3p	1.506	1.143	0.206194	0.540094
hsa-miR-181a-5p-477857-mir	hsa-miR-181a-5p	-0.7025	1.214	0.570892	0.861366
hsa-miR-181b-5p-478583-mir	hsa-miR-181b-5p	4.036	1.421	0.011813	0.119905
hsa-miR-181c-5p-477934-mir	hsa-miR-181c-5p	-0.932	1.526	0.550072	0.861366
hsa-miR-182-5p-477935-mir	hsa-miR-182-5p	1.343	2.965	0.656734	0.882403
hsa-miR-185-3p-478732-mir	hsa-miR-185-3p	4.478	2.024	0.041805	0.242655
hsa-miR-185-5p-477939-mir	hsa-miR-185-5p	-0.6215	0.5307	0.258722	0.607332
hsa-miR-186-5p-477940-mir	hsa-miR-186-5p	0.2165	1.377	0.876993	0.956954
hsa-miR-18a-5p-478551-mir	hsa-miR-18a-5p	-0.5	0.3393	0.159999	0.48976
hsa-miR-18b-5p-478584-mir	hsa-miR-18b-5p	0.312	2.033	0.879958	0.956954
hsa-miR-190a-5p-478358-mir	hsa-miR-190a-5p	-4.752	1.278	0.001869	0.045536
hsa-miR-191-5p-477952-mir	hsa-miR-191-5p	-1.493	0.5731	0.019142	0.150422
hsa-miR-192-5p-478262-mir	hsa-miR-192-5p	-1.728	1.506	0.268157	0.607332
hsa-miR-193a-5p-477954-mir	hsa-miR-193a-5p	-1.767	2.293	0.452228	0.781777
hsa-miR-193b-3p-478314-mir	hsa-miR-193b-3p	-0.91	2.214	0.68647	0.882403
hsa-miR-194-5p-477956-mir	hsa-miR-194-5p	-2.243	1.672	0.198523	0.537334
hsa-miR-195-5p-477957-mir	hsa-miR-195-5p	-0.6385	0.2816	0.037571	0.240848
hsa-miR-197-3p-477959-mir	hsa-miR-197-3p	-0.221	4.788	0.963754	0.986431
hsa-miR-199a-3p-477961-mir	hsa-miR-199a-3p	7.243	1.029	0.000003	0.000684
hsa-miR-199a-5p-478231-mir	hsa-miR-199a-5p	-3.371	1.76	0.073546	0.32987
hsa-miR-199b-5p-478486-mir	hsa-miR-199b-5p	-1.066	2.781	0.706653	0.882403
hsa-miR-19a-3p-479228-mir	hsa-miR-19a-3p	0.3625	0.6735	0.597844	0.87385
hsa-miR-19b-3p-478264-mir	hsa-miR-19b-3p	-1.205	1.394	0.400488	0.750453
hsa-miR-205-5p-477967-mir	hsa-miR-205-5p	-7.469	2.594	0.010897	0.119905
hsa-miR-208a-3p-477819-mir	hsa-miR-208a-3p	1.828	2.31	0.440396	0.781777
hsa-miR-208b-3p-477806-mir	hsa-miR-208b-3p	5.953	1.453	0.000842	0.0293
hsa-miR-20a-5p-478586-mir	hsa-miR-20a-5p	-0.617	0.4651	0.2033	0.538302
hsa-miR-20b-5p-477804-mir	hsa-miR-20b-5p	-0.201	2.643	0.940311	0.983089
hsa-miR-21-5p-477975-mir	hsa-miR-21-5p	-1.185	0.5077	0.032961	0.217007
hsa-miR-210-3p-477970-mir	hsa-miR-210-3p	1.43	1.792	0.436637	0.781777
hsa-miR-215-5p-478516-mir	hsa-miR-215-5p	1.621	2.453	0.518112	0.84706
hsa-miR-22-3p-477985-mir	hsa-miR-22-3p	-0.543	0.5657	0.351423	0.713388
hsa-miR-22-5p-477987-mir	hsa-miR-22-5p	1.91	1.38	0.18551	0.51884
hsa-miR-221-3p-477981-mir	hsa-miR-221-3p	-1.326	0.464	0.011427	0.119905
hsa-miR-222-3p-477982-mir	hsa-miR-222-3p	-0.2975	1.228	0.811648	0.946017
hsa-miR-223-3p-477983-mir	hsa-miR-223-3p	-1.949	0.807	0.028057	0.201018
hsa-miR-223-5p-477984-mir	hsa-miR-223-5p	-3.926	1.794	0.043829	0.242655
hsa-miR-23a-3p-478532-mir	hsa-miR-23a-3p	0.7455	0.6853	0.292784	0.632944
hsa-miR-23b-3p-478602-mir	hsa-miR-23b-3p	3.408	2.422	0.178494	0.51884

hsa-miR-24-1-5p-478784-mir	hsa-miR-24-1-5p	-2.027	1.466	0.185651	0.51884
hsa-miR-24-3p-477992-mir	hsa-miR-24-3p	-0.304	0.6826	0.662015	0.882403
hsa-miR-25-3p-477994-mir	hsa-miR-25-3p	-0.309	0.201	0.143829	0.456142
hsa-miR-26a-5p-477995-mir	hsa-miR-26a-5p	-1.555	0.6987	0.040776	0.242655
hsa-miR-26b-5p-478418-mir	hsa-miR-26b-5p	-1.635	0.5383	0.00784	0.100523
hsa-miR-27a-3p-478384-mir	hsa-miR-27a-3p	1.406	2.231	0.53752	0.859543
hsa-miR-27b-3p-478270-mir	hsa-miR-27b-3p	3.062	1.907	0.12782	0.451816
hsa-miR-28-3p-477999-mir	hsa-miR-28-3p	-1.156	1.845	0.539861	0.859543
hsa-miR-28-5p-478000-mir	hsa-miR-28-5p	-1.167	2.291	0.617369	0.874367
hsa-miR-296-3p-478790-mir	hsa-miR-296-3p	-0.616	3.747	0.871461	0.956954
hsa-miR-29a-3p-478587-mir	hsa-miR-29a-3p	-1.045	0.7434	0.178936	0.51884
hsa-miR-29a-5p-478002-mir	hsa-miR-29a-5p	-3.419	2.439	0.180183	0.51884
hsa-miR-29b-3p-478369-mir	hsa-miR-29b-3p	-0.8855	0.4629	0.073807	0.32987
hsa-miR-29c-3p-479229-mir	hsa-miR-29c-3p	-0.985	0.485	0.059213	0.301211
hsa-miR-29c-5p-478005-mir	hsa-miR-29c-5p	-1.719	1.491	0.265812	0.607332
hsa-miR-301a-3p-477815-mir	hsa-miR-301a-3p	-2.712	1.733	0.137251	0.451816
hsa-miR-301b-3p-477825-mir	hsa-miR-301b-3p	-3.858	1.411	0.014684	0.137582
hsa-miR-30a-5p-479448-mir	hsa-miR-30a-5p	5.94	2.926	0.059352	0.301211
hsa-miR-30b-5p-478007-mir	hsa-miR-30b-5p	1.051	2.013	0.608962	0.87385
hsa-miR-30c-5p-478008-mir	hsa-miR-30c-5p	-1.199	0.7805	0.144183	0.456142
hsa-miR-30d-5p-478606-mir	hsa-miR-30d-5p	-0.1355	0.6478	0.836954	0.95272
hsa-miR-30e-3p-478388-mir	hsa-miR-30e-3p	-2.548	2.674	0.35483	0.714351
hsa-miR-30e-5p-479235-mir	hsa-miR-30e-5p	-0.7325	0.9431	0.448675	0.781777
hsa-miR-32-5p-478026-mir	hsa-miR-32-5p	-2.15	3.311	0.525408	0.850167
hsa-miR-320a-478594-mir	hsa-miR-320a	-0.2775	0.5644	0.629598	0.882145
hsa-miR-320b-478588-mir	hsa-miR-320b	4.309	1.967	0.04362	0.242655
hsa-miR-324-3p-478023-mir	hsa-miR-324-3p	0.898	2.715	0.745081	0.894098
hsa-miR-324-5p-478024-mir	hsa-miR-324-5p	-0.6005	1.488	0.69189	0.882403
hsa-miR-326-478027-mir	hsa-miR-326	-2.69	2.384	0.275731	0.61073
hsa-miR-328-3p-478028-mir	hsa-miR-328-3p	-2.401	2.055	0.259884	0.607332
hsa-miR-329-3p-478029-mir	hsa-miR-329-3p	0.68	1.796	0.709968	0.882403
hsa-miR-330-5p-478830-mir	hsa-miR-330-5p	3.39	3.122	0.293607	0.632944
hsa-miR-331-3p-478323-mir	hsa-miR-331-3p	-0.8395	2.436	0.73488	0.888988
hsa-miR-335-5p-478324-mir	hsa-miR-335-5p	1.591	1.84	0.400088	0.750453
hsa-miR-337-5p-478036-mir	hsa-miR-337-5p	-1.488	2.118	0.492511	0.821752
hsa-miR-338-3p-478037-mir	hsa-miR-338-3p	-2.947	2.272	0.212954	0.551868
hsa-miR-339-3p-478325-mir	hsa-miR-339-3p	2.896	1.822	0.131488	0.451816
hsa-miR-339-5p-478040-mir	hsa-miR-339-5p	-0.9155	1.528	0.557421	0.861366
hsa-miR-33a-5p-478347-mir	hsa-miR-33a-5p	0.1305	1.895	0.945961	0.984506
hsa-miR-33b-5p-478479-mir	hsa-miR-33b-5p	0.83	2.123	0.700983	0.882403
hsa-miR-340-3p-478041-mir	hsa-miR-340-3p	-0.1375	2.272	0.952485	0.984506
hsa-miR-340-5p-478042-mir	hsa-miR-340-5p	1.255	1.483	0.409912	0.756473
hsa-miR-342-3p-478043-mir	hsa-miR-342-3p	-1.024	1.455	0.49196	0.821752
hsa-miR-345-5p-478366-mir	hsa-miR-345-5p	0.67	2.326	0.777054	0.920052
hsa-miR-34a-5p-478048-mir	hsa-miR-34a-5p	4.255	1.272	0.004116	0.066138
hsa-miR-361-3p-478055-mir	hsa-miR-361-3p	-0.0155	1.849	0.993416	0.999984
hsa-miR-361-5p-478056-mir	hsa-miR-361-5p	0.6095	1.546	0.698618	0.882403
hsa-miR-363-3p-478060-mir	hsa-miR-363-3p	-0.235	0.4037	0.568555	0.861366
hsa-miR-365a-3p-478065-mir	hsa-miR-365a-3p	-5.157	2.074	0.02433	0.179603
hsa-miR-369-3p-478067-mir	hsa-miR-369-3p	1.197	1.851	0.526992	0.850167
hsa-miR-374a-3p-478855-mir	hsa-miR-374a-3p	-6.191	1.454	0.0006	0.028177
hsa-miR-374b-5p-478389-mir	hsa-miR-374b-5p	2.243	1.175	0.074478	0.32987
hsa-miR-375-478074-mir	hsa-miR-375	-2.386	2.648	0.380997	0.736595
hsa-miR-376c-3p-478459-mir	hsa-miR-376c-3p	-1.558	1.912	0.42722	0.781777
hsa-miR-377-3p-478075-mir	hsa-miR-377-3p	0.4705	2.227	0.835336	0.95272

hsa-miR-378a-3p-478349-mir	hsa-miR-378a-3p	0.5415	1.489	0.720846	0.882403
hsa-miR-380-3p-477854-mir	hsa-miR-380-3p	-2.863	2.452	0.260197	0.607332
hsa-miR-409-3p-478084-mir	hsa-miR-409-3p	-2.259	2.068	0.290841	0.632944
hsa-miR-410-3p-478085-mir	hsa-miR-410-3p	-2.199	2.491	0.390429	0.744907
hsa-miR-423-3p-478327-mir	hsa-miR-423-3p	0.2235	1.83	0.904316	0.962916
hsa-miR-423-5p-478090-mir	hsa-miR-423-5p	1.639	1.533	0.300871	0.637322
hsa-miR-424-3p-478091-mir	hsa-miR-424-3p	-3.148	1.782	0.096332	0.384696
hsa-miR-424-5p-478092-mir	hsa-miR-424-5p	-1.125	0.6587	0.107133	0.407776
hsa-miR-425-3p-478093-mir	hsa-miR-425-3p	1.318	1.747	0.461604	0.786341
hsa-miR-425-5p-478094-mir	hsa-miR-425-5p	-0.7935	0.5959	0.201645	0.538302
hsa-miR-432-5p-478101-mir	hsa-miR-432-5p	0.75	1.528	0.630104	0.882145
hsa-miR-450a-5p-478106-mir	hsa-miR-450a-5p	-0.8815	1.96	0.658899	0.882403
hsa-miR-450b-3p-478913-mir	hsa-miR-450b-3p	-2.753	3.247	0.408985	0.756473
hsa-miR-450b-5p-478914-mir	hsa-miR-450b-5p	0.643	1.736	0.715886	0.882403
hsa-miR-451a-478107-mir	hsa-miR-451a	1.036	0.4355	0.030241	0.210478
hsa-miR-452-3p-478917-mir	hsa-miR-452-3p	-7.666	2.676	0.011232	0.119905
hsa-miR-483-5p-478432-mir	hsa-miR-483-5p	0.498	2.474	0.842988	0.955125
hsa-miR-484-478308-mir	hsa-miR-484	-1.164	0.3367	0.003243	0.056422
hsa-miR-485-3p-478125-mir	hsa-miR-485-3p	-4.37	2.18	0.062276	0.308448
hsa-miR-486-3p-478422-mir	hsa-miR-486-3p	-0.2865	2.419	0.907191	0.962916
hsa-miR-486-5p-478128-mir	hsa-miR-486-5p	0.007	0.4883	0.98874	0.999646
hsa-miR-487a-3p-477826-mir	hsa-miR-487a-3p	4.349	3.583	0.242471	0.607332
hsa-miR-487b-3p-477835-mir	hsa-miR-487b-3p	2.354	1.703	0.185944	0.51884
hsa-miR-490-3p-478131-mir	hsa-miR-490-3p	-3.293	4.307	0.455716	0.781777
hsa-miR-494-3p-478135-mir	hsa-miR-494-3p	-2.588	2.258	0.268561	0.607332
hsa-miR-495-3p-478136-mir	hsa-miR-495-3p	2.209	1.861	0.252577	0.607332
hsa-miR-497-5p-478138-mir	hsa-miR-497-5p	2.442	1.33	0.084957	0.356819
hsa-miR-499a-5p-478139-mir	hsa-miR-499a-5p	5.435	1.297	0.000694	0.028177
hsa-miR-500a-3p-478951-mir	hsa-miR-500a-3p	-0.96	1.863	0.613417	0.87385
hsa-miR-502-3p-478348-mir	hsa-miR-502-3p	3.399	1.24	0.014525	0.137582
hsa-miR-503-5p-478143-mir	hsa-miR-503-5p	-1.582	1.618	0.342822	0.707723
hsa-miR-505-3p-478145-mir	hsa-miR-505-3p	-1.093	1.878	0.56875	0.861366
hsa-miR-516b-5p-478979-mir	hsa-miR-516b-5p	-2.386	2.301	0.315213	0.661948
hsa-miR-525-3p-478995-mir	hsa-miR-525-3p	0.8805	1.934	0.655032	0.882403
hsa-miR-532-3p-478336-mir	hsa-miR-532-3p	0.1265	2.275	0.956353	0.984506
hsa-miR-532-5p-478151-mir	hsa-miR-532-5p	-0.177	1.645	0.915639	0.965583
hsa-miR-542-3p-478153-mir	hsa-miR-542-3p	2.018	1.744	0.264272	0.607332
hsa-miR-548a-3p-478157-mir	hsa-miR-548a-3p	0.354	1.539	0.82098	0.952337
hsa-miR-548d-5p-480870-mir	hsa-miR-548d-5p	1.065	3.007	0.727798	0.886459
hsa-miR-548n-479024-mir	hsa-miR-548n	-0.864	2.327	0.715263	0.882403
hsa-miR-550a-3p-479032-mir	hsa-miR-550a-3p	4.473	2.595	0.104017	0.407776
hsa-miR-550a-5p-477852-mir	hsa-miR-550a-5p	-2.401	4.032	0.55988	0.861366
hsa-miR-551a-478158-mir	hsa-miR-551a	-2.057	2.65	0.449006	0.781777
hsa-miR-551b-3p-478159-mir	hsa-miR-551b-3p	-3.744	2.252	0.115965	0.421629
hsa-miR-562-479047-mir	hsa-miR-562	-1.968	2.476	0.438498	0.781777
hsa-miR-576-5p-478165-mir	hsa-miR-576-5p	-0.508	1.162	0.667864	0.882403
hsa-miR-582-5p-478166-mir	hsa-miR-582-5p	-2.728	2.003	0.192091	0.525768
hsa-miR-584-5p-478167-mir	hsa-miR-584-5p	-0.4265	2.036	0.83675	0.95272
hsa-miR-585-3p-479067-mir	hsa-miR-585-3p	-1.316	3.111	0.677914	0.882403
hsa-miR-590-3p-478168-mir	hsa-miR-590-3p	-2.588	1.629	0.131745	0.451816
hsa-miR-590-5p-478367-mir	hsa-miR-590-5p	-2.163	1.89	0.269261	0.607332
hsa-miR-598-3p-478172-mir	hsa-miR-598-3p	0.161	1.389	0.909157	0.962916
hsa-miR-616-3p-478177-mir	hsa-miR-616-3p	-0.4465	3.13	0.888337	0.957517
hsa-miR-624-5p-478178-mir	hsa-miR-624-5p	0.308	1.924	0.874834	0.956954
hsa-miR-625-5p-479469-mir	hsa-miR-625-5p	-2.269	2.364	0.351334	0.713388

hsa-miR-628-3p-478181-mir	hsa-miR-628-3p	4.44	1.895	0.032355	0.217007
hsa-miR-629-5p-478183-mir	hsa-miR-629-5p	-3.882	1.772	0.043642	0.242655
hsa-miR-633-479115-mir	hsa-miR-633	-0.7785	1.822	0.67483	0.882403
hsa-miR-651-5p-479131-mir	hsa-miR-651-5p	-0.618	2.208	0.783188	0.921665
hsa-miR-652-3p-478189-mir	hsa-miR-652-3p	-0.251	0.5729	0.667156	0.882403
hsa-miR-653-5p-479134-mir	hsa-miR-653-5p	1.124	2.007	0.583396	0.861366
hsa-miR-654-3p-479135-mir	hsa-miR-654-3p	-2.561	2.756	0.366649	0.726143
hsa-miR-656-3p-479137-mir	hsa-miR-656-3p	0.1795	2.234	0.936957	0.983089
hsa-miR-660-5p-478192-mir	hsa-miR-660-5p	3.963	1.332	0.008946	0.108967
hsa-miR-664a-3p-478193-mir	hsa-miR-664a-3p	-0.021	1.496	0.988977	0.999646
hsa-miR-671-3p-478194-mir	hsa-miR-671-3p	-8.201	1.851	0.00042	0.026109
hsa-miR-7-1-3p-478198-mir	hsa-miR-7-1-3p	0.964	1.87	0.613305	0.87385
hsa-miR-7-2-3p-478199-mir	hsa-miR-7-2-3p	-0.648	2.938	0.828231	0.95272
hsa-miR-7-5p-478341-mir	hsa-miR-7-5p	-1.147	1.221	0.361625	0.722065
hsa-miR-744-5p-478200-mir	hsa-miR-744-5p	-1.162	1.71	0.506434	0.833563
hsa-miR-758-3p-479166-mir	hsa-miR-758-3p	0.762	1.895	0.692995	0.882403
hsa-miR-874-3p-478205-mir	hsa-miR-874-3p	-3.553	2.407	0.159334	0.48976
hsa-miR-885-5p-478207-mir	hsa-miR-885-5p	1.01	2.168	0.647526	0.882403
hsa-miR-92a-3p-477827-mir	hsa-miR-92a-3p	-0.597	0.2199	0.01529	0.137951
hsa-miR-92b-3p-477823-mir	hsa-miR-92b-3p	-0.6615	0.3917	0.11063	0.408323
hsa-miR-93-3p-478209-mir	hsa-miR-93-3p	-1.346	1.528	0.391413	0.744907
hsa-miR-93-5p-478210-mir	hsa-miR-93-5p	-0.562	1.001	0.582226	0.861366
hsa-miR-937-3p-479212-mir	hsa-miR-937-3p	-3.259	4.255	0.454942	0.781777
hsa-miR-96-5p-478215-mir	hsa-miR-96-5p	-0.72	1.383	0.60978	0.87385
hsa-miR-98-5p-478590-mir	hsa-miR-98-5p	0.963	3.011	0.753241	0.899459
hsa-miR-99a-3p-479224-mir	hsa-miR-99a-3p	-0.259	1.48	0.863265	0.95587
hsa-miR-99a-5p-478519-mir	hsa-miR-99a-5p	0.7985	2.338	0.737174	0.888988
hsa-miR-99b-5p-478343-mir	hsa-miR-99b-5p	-2.779	2.018	0.18743	0.51884